JPET Fast Forward. Published on October 11, 2017 as DOI: 10.1124/jpet.117.240507
This article has not been copyedited and formatted. The final version may differ from this version.

Activation of FAK and Src mediates acquired sorafenib resistance in A549 human lung adenocarcinoma xenografts

Qingyu Zhou, Xiaofang Guo, Riya Choksi

Department of Pharmaceutical Sciences, College of Pharmacy, University of South Florida, Tampa, FL 33612 (Q.Z., X.G., R.C.)

Running title: FAK/Src activation mediates acquired sorafenib resistance

Corresponding author: Qingyu Zhou

Current address: Department of Pharmaceutical Sciences, College of Pharmacy, University of South Florida, Tampa, FL 33612. E-mail: qzhou1@health.usf.edu

Number of text pages:

Number of tables: 1

Number of figures: 6

Number of references: 50

Number of words in the Abstract: 241

Number of words in the Introduction: 750

Number of words in the Discussion: 1495

Nonstandard abbreviations: ABCG2, ATP-binding cassette sub-family G member 2; AKT, protein kinase B; BATTLE, biomarker-integrated approaches of targeted therapy for lung cancer elimination; CI, combination index; c-Kit, stem cell factor receptor; DCR, disease control rate; DMEM, Dulbecco's Modified Eagle's media; DMSO, dimethyl sulfoxide; EGFR, epidermal growth factor receptor; EMT, epithelial-mesenchymal transition; ERK1/2, extracellular signal-regulated protein kinases 1 and 2; FAK, focal adhesion kinase; FGF, fibroblast growth factor; FGFR-1, fibroblast growth factor receptor 1; GSK3α/β, glycogen synthase kinases 3α and 3β; HCC, hepatocellular carcinoma; HGF, hepatocyte growth factor; HPLC, high-performance liquid

chromatography; IGF, insulin-like growth factor; IS, internal standard; LLOQ, lower limits of quantitation; MAPK, mitogen-activated protein kinase; MCL-1, myeloid cell leukemia sequence 1 protein; MMP9, matrix metallopeptidase 9; MT-1G, metallothionein-1G; mTOR, mechanistic target of rapamycin; MTT, 3-[4,5-dimethylthiazole-2-yl]-2,5-diphenyl-tetrazolium bromide; NSCLC, non-small cell lung cancer; STAT3, signal transducer and activator of transcription 3; PBS, phosphate buffered saline; RSK, 90 kDa ribosomal S6 kinase; PDGFR, platelet-derived growth factor receptor; SEM, standard error of mean; VEGFR, vascular endothelial growth factor receptor;

Section: Chemotherapy, Antibiotics, and Gene Therapy

Abstract

Despite encouraging clinical results with sorafenib monotherapy in patients with *KRAS*-mutant non-small cell lung cancer (NSCLC), the overall survival benefit of this drug is limited by the inevitable development of acquired resistance. The exact mechanism underlying acquired sorafenib resistance in *KRAS*-mutant NSCLC is unclear. In this study, the mechanism of acquired sorafenib resistance was explored using a biologically relevant xenograft model, which was established by using the A549 human lung adenocarcinoma cell line and an *in-vivo* derived sorafenib-resistant A549 subline (A549/SRFres). Results from the initial study demonstrated that sorafenib treatment significantly decreased E-cadherin ($P<0.05$) levels but significantly increased MMP9 levels ($P<0.01$) in A549/SRFres tumors, while expression levels of phospho-AKT, phospho-FAK and phospho-Src were elevated in sorafenib-treated A549 and A549/SRFres tumors. We next examined if the concomitant dasatinib treatment could overcome acquired sorafenib resistance by blocking the FAK/Src escape route that mediates the resistance. Despite the observed *in-vitro* synergy between sorafenib and dasatinib, the *in-vivo* anti-tumor effect of half-dose sorafenib-dasatinib combination therapy was inferior to that of the full-dose sorafenib treatment. Although the sorafenib-dasatinib combination effectively inhibited Src and AKT phosphorylation, it did not block the Y576/577-FAK phosphorylation nor decreased vimentin protein expression, but unexpectedly increased the Y397-FAK phosphorylation and MMP9 protein expression in tumors. These results suggest that acquired sorafenib resistance in *KRAS*-mutant A549 xenografts involves the compensatory activation of FAK and Src, and Src

inhibition alone is insufficient to diminish sorafenib-promoted epithelial-mesenchymal transition (EMT) process and invasive potentials in tumors.

Introduction

Over the past two decades, the therapeutic landscape of advanced cancer has been revolutionized by the rapid development of molecularly targeted therapy. With the increasing use of targeted therapeutic agents came the challenge of addressing the inevitable development of acquired drug resistance. In the field of targeted therapy in NSCLC, much effort has focused on developing inhibitors of epidermal growth factor receptor (EGFR) as the first-line treatment for patients with activating EGFR mutations (Pao and Chmielecki, 2010), and identifying mechanisms of acquired resistance to the EGFR inhibitors so that therapeutic approaches can be developed to overcome the resistance (Wheeler et al., 2010). Besides *EGFR* mutations, the aberrant activation of the RAS/RAF/MEK/ERK pathway via activating mutations in *KRAS* also occurs frequently in NSCLC, mainly adenocarcinomas (Gotz, 2008). It has been reported that the prevalence of patients with *KRAS*-mutant NSCLC is approximately 15% (Chan and Hughes, 2015). Since direct inhibition of KRAS remains therapeutically challenging, an alternative approach for treating *KRAS*-mutant NSCLC that has been pursued is to target signaling pathways downstream of RAS. In this regard, several recent clinical trials have been conducted to examine the efficacy of sorafenib, a multikinase inhibitor targeting the RAF/MEK/ERK pathway and the vascular endothelial growth factor receptors (VEGFRs) and platelet-derived growth factor receptors (PDGFRs) (Wilhelm et al., 2006), in the treatment of NSCLC.

In the BATTLE (biomarker-integrated approaches of targeted therapy for lung cancer elimination) trial, which was designed to evaluate the effectiveness of small molecule kinase inhibitors in patients with chemorefractory NSCLC based on relevant molecular

biomarkers (Kim et al., 2011), sorafenib treatment resulted in a better-than-average overall 8-week disease control rate (DCR) (58% versus 46%) in the *KRAS*/*BRAF*, *VEGF*/*VEGFR-2* and no-marker groups. More strikingly, sorafenib had a 79% DCR compared to a 14% DCR with erlotinib in the *KRAS*/*BRAF* marker group (Kim et al., 2011). However, results from the Phase 3 MISSION trial, in which sorafenib was used as a single agent in patients with advanced relapsed or refractory NSCLC, indicated that sorafenib monotherapy did not improve the overall survival in spite of a statistically significant improvement of several secondary endpoints including progression-free survival and time to disease progression (Paz-Ares et al., 2015). Collectively, those clinical data suggest that the initial treatment with sorafenib is efficacious, but resistance to the drug is eventually developed. Given the acquired resistance being a major factor that limits the clinical success of sorafenib therapy in patients with *KRAS*-mutant NSCLC, understanding the molecular mechanisms underlying the resistance will be crucial for maximizing the therapeutic outcome.

Acquired sorafenib resistance has been associated with the activation of bypass signaling driven by alternative receptor tyrosine kinases. A diversity of adaptive molecular events underpinning the resistance have been reported under different experimental conditions, including the induction of metallothionein-1G (MT-1G) (Sun et al., 2016) and the activation of parallel pathways that promote the malignant properties of the tumor, such as the protein kinase B (AKT) pathway (Chen et al., 2011; Morgillo et al., 2011; Lindblad et al., 2016), the mitogen-activated protein kinase (MAPK) pathway (Morgillo et al., 2011; Harada et al., 2014), the signal transducer and activator of transcription 3 (STAT3) pathway (Tai et al., 2012), the hepatocyte growth factor

(HGF)/c-Met pathway (Firtina Karagonlar et al., 2016), and the insulin-like growth factor (IGF)/fibroblast growth factor (FGF) pathway (Tovar et al., 2015).

In the present study, we sought to examine the molecular mechanisms by which NSCLC adapts to evade sorafenib therapy using a biologically relevant xenograft model of acquired sorafenib resistance, and to translate the knowledge into a combinatorial therapy option comprised of sorafenib and dasatinib in hopes of increasing the antitumor efficacy of sorafenib against tumors with acquired resistance to sorafenib, and to elucidate underlying mechanisms of interaction between sorafenib and dasatinib. Dasatinib is a potent kinase inhibitor targeting multiple protein kinases, including, Bcr-Abl, Src, stem cell factor receptor (c-Kit), fibroblast growth factor receptor 1 (FGFR-1) and PDGFRβ (Kantarjian et al., 2006). Combination therapy with sorafenib and dasatinib for the treatment of NSCLC has not been described so far. By using an A549 human lung adenocarcinoma xenograft model, we were able to explore the mechanisms of acquired sorafenib resistance in the context of tumor microenvironment, which is known to contribute substantially to the acquisition of tumor resistance to targeted therapies (McMillin et al., 2013). The goal of this investigation is not only to gain a broader understanding of acquired sorafenib resistance in NSCLC, but also to provide a framework for the rational design of targeted combinatorial therapy that can effectively manage such resistance.

Materials and Methods

Reagents

Sorafenib base, sorafenib tosylate and dasatinib base were purchased from LC Laboratories (Woburn, MA). For the *in vitro* study, sorafenib base and dasatinib base

were dissolved in dimethyl sulfoxide (DMSO). To prepare the stock solutions for the *in vivo* study, sorafenib tosylate was dissolved in Cremophor EL/ethanol (50:50, v/v) at 4× concentration, and dasatinib base was dissolved in propylene glycol at 2× concentration. The stock solutions were prepared fresh every 3 days. The final dosing solution was prepared by diluting the stock solution to 1× concentration with sterile water. All other chemicals, solvents and reagents were obtained from commercial sources.

Animals

Male athymic nude mice (Hsd: Athymic Nude-*Foxn1*^{nu}; 6-8 weeks old) were purchased from Envigo (Indianapolis, IN). All animal experiments were approved by the Institutional Animal Care and Use Committee and performed according to the NIH guidelines.

Cell Line, Sorafenib-Resistant Subclone and Culture Condition

The A549 human lung adenocarcinoma cell line (ATCC® CCL-185™) was purchased from the American Type Culture Collection (Manassas, VA). The sorafenib-resistant A549 subclone (A549/SRFres) was derived from a sorafenib-treated animal with the fastest growing A549 xenograft. Both parental A549 and A549/SRFres cells were cultured in a mixture of Dulbecco's Modified Eagle's Media (DMEM)/Ham's F12 at a ratio of 1:1 (Mediatech Inc. Herndon, VA) supplemented with 10% fetal bovine serum (Sigma-Aldrich, St. Louis, MO), 100 units/mL penicillin, and 100 µg/mL streptomycin, and maintained in a humidified atmosphere of 5% CO_2 in air at 37°C. All experiments

were conducted using A549 and A549/SRFres cells with passage number less than 20 and 10, respectively.

In-Vivo Sorafenib-Resistant A549 Xenograft Model

Initial Model Development Protocol Parental A549 tumor cells (5×10^6) suspended in 0.2 ml Matrigel (BD Biosciences) were injected subcutaneously into the left flank of the athymic nude mice. Tumor-bearing mice were randomly divided into control (N = 9) and sorafenib (N = 10) groups. Seven days after tumor inoculation, each animal was given once-daily oral administration of either vehicle or sorafenib on a 6-day-on/1-day-off schedule for 15 consecutive weeks. Sorafenib was given at a dose of 10 mg/kg/d for the 1st week, 20 mg/kg/d for the 2nd week and 40 mg/kg/d from the 3rd week onward. Tumor growth was monitored once a week using a digital caliper (Fisher Scientific) with the volume calculated as $0.5 \times \text{length} \times \text{width}^2$. Phenotypic sensitivity of individual mice to sorafenib treatment was defined based on the degree of suppression of tumor growth, which was expressed as the tumor growth index (*i.e*. the ratio of tumor volume on the last day to that on the first day of the treatment).

In Vivo Study Protocol Each animal was inoculated subcutaneously with A549 and A549/SRFres cells (5×10^6 each) on the left and right flanks, respectively (Fig.1C). Seven days after tumor inoculation, tumor-bearing animals were randomly divided into control (N = 6) and sorafenib (N = 7) groups. Each animal received once-daily oral administration of vehicle control or sorafenib on a 6-day-on/1-day-off schedule for 8 – 12 consecutive weeks. Sorafenib dose escalation scheme was the same as that described above. Tumor growth was determined as described above. All animals were

JPET Fast Forward. Published on October 11, 2017 as DOI: 10.1124/jpet.117.240507
This article has not been copyedited and formatted. The final version may differ from this version.

euthanized with CO_2 gas at the end of the treatment period. The tumor mass was excised, snap frozen on dry ice and stored at –80^{o}C before subjected to Western blot analysis.

In Vitro Comparison of Doubling Time between A549 and A549/SRFres Cells

See the Supplemental Methods for a detailed description of the experiment.

Wound-Healing Assay

See the Supplemental Methods for a detailed description of the assay.

Cell Invasion Assay

See the Supplemental Methods for a detailed description of the assay.

In Vitro Cytotoxicity Assay

Cytotoxicity was analyzed using the MTT (3-[4,5-dimethylthiazole-2-yl]-2,5-diphenyl-tetrazolium bromide) assay. Briefly, A549 and A549/SRFres cells were seeded in 96-well plates at a density of 3×10^3 cells/well and allowed to attach overnight. On the next day, culture media containing either vehicle control (0.5% DMSO), sorafenib (13 nM – 100 μM), dasatinib (13 nM – 100 μM) or the combination of sorafenib and dasatinib (6 nM – 50 μM for each drug) were added to appropriate wells. The molar ratios of sorafenib to dasatinib were fixed at 1:1, 3:1 and 1:3. After the cells were treated for 72 hours, 5 μl of 5 mg/ml of MTT in PBS was added to each well and individual plates was incubated for 2 hours at 37 ^{o}C following by the addition of 100 μl of DMAO to each well and incubation at room temperature in the dark for 2 more hours. Optical densities were measured at 570 nm with a SpectraMax 190 microplate reader equipped with SoftMax

JPET Fast Forward. Published on October 11, 2017 as DOI: 10.1124/jpet.117.240507
This article has not been copyedited and formatted. The final version may differ from this version.

Pro software (Molecular Devices, Sunnyvale, CA). The growth of treated cells was expressed as a percentage of vehicle control cultures. Concentrations of individual drugs required for 50% inhibition of cell growth (*i.e.*, IC_{50}) as compared with the control cells were calculated by nonlinear fitting of the experimental data obtained from multiple independent experiments performed in duplicates or triplicates using the GraphPad Prism 5.0 program (GraphPad Software, Inc. La Jolla, CA). The combination effects of sorafenib and dasatinib was further evaluated based on the combination index (CI) values (Chou and Talalay, 1981).

In Vivo Evaluation of Combination Therapy with Sorafenib and Dasatinib

Three weeks after individual athymic nude mice were injected subcutaneously with A549 and A549/SRFres cells (5×10^6) on the left and right franks, respectively, those tumor-bearing animals were randomly divided into four groups: (1) vehicle control (N = 7), (2) full-dose sorafenib (40 mg/kg/d, N = 7), (3) full-dose dasatinib (40 mg/kg/d, N = 8), and (4) half-dose combination (20 mg/kg/d of sorafenib and 20 mg/kg of dasatinib, N = 8) groups. Individual animals were given once daily oral administration of either vehicle or therapeutic agents for 28 consecutive days. Body weight and tumor volume were measured twice a week throughout the treatment period. On the last day of the treatment period, 4 hours after the last dose, individual animals were sedated with isoflurane and euthanized with terminal bleeding from vena cava. Plasma was separated by centrifugation and then stored at -80 ^oC before subjected to drug analysis using the high-performance liquid chromatography (HPLC). The tumor mass was immediately excised, snap frozen on dry ice, and stored at –80^oC before subjected to drug analysis, Western blot analysis and immunofluorescence double staining.

JPET Fast Forward. Published on October 11, 2017 as DOI: 10.1124/jpet.117.240507
This article has not been copyedited and formatted. The final version may differ from this version.

Immunofluorescence Double Staining

Frozen A549 and A549/SRFres tumor samples were cryosectioned at a thickness of 10 μm, and then subjected to immunofluorescence double staining as described previously (Zhou et al., 2012). The primary antibodies used included rabbit anti-mouse collagen type IV antibody (1:100, EMD Millipore), rabbit monoclonal antibody anti-E-cadherin (1:100, Cell Signaling Technologies, Danvers, MA), rabbit monoclonal anti-Ki-67 (1:100, Abcam, Cambridge, MA), rabbit polyclonal anti-α-smooth muscle actin (α-SMA) (1:100, Abcam), and rat monoclonal anti-CD31 (1:200, BD Pharmingen, San Jose, CA). Secondary antibodies were Alexa Fluor 594 conjugated goat anti-rabbit IgG and Alexa Fluor 488 conjugated goat anti-rat IgG (1:200 for each, Thermo Fisher Scientific), which generate red and green fluorescence, respectively. Sections were mounted with ProLong Gold Antifade Reagent with DAPI (Life Technologies), and analyzed under an Olympus BX53 digital fluorescence microscope. Images were processed using the ImageJ 1.47 software (from NIH and available at http://rsb.info.nih.gov/ij/).

Western Blot Analysis

In vitro cultured parental A549 and A549/SRFres cells that were treated with vehicle (0.5% DMSO), sorafenib (10 μM) and dasatinib (0.2 μM or 0.02 μM) alone or in combination for 4 hours, and tumor tissue samples collected from the *in vivo* studies were subjected to Western blot analysis. Cell lysate samples and tumor tissue lysate samples were prepared as previously described (Zhou et al., 2008). Immunoblotting was carried out with the following primary antibodies: rabbit polyclonal antibodies from Abcam: ATP-binding cassette sub-family G member 2 (ABCG2; 1:1000), α-SMA

JPET Fast Forward. Published on October 11, 2017 as DOI: 10.1124/jpet.117.240507
This article has not been copyedited and formatted. The final version may differ from this version.

(1:1000), matrix metallopeptidase 9 (MMP9; 1:5000); rabbit polyclonal or monoclonal antibodies from Cell Signaling Technologies (1:1000 dilution for all): AKT (pan), phosphor-AKT (S473), extracellular signal-regulated protein kinases 1 and 2 (ERK1/2), phospho-ERK1/2 (T202/Y204), focal adhesion kinase (FAK), phospho-FAK (Y397). Phospho-FAK(Y576/577), Glycogen synthase kinases 3α and 3β (GSK3α/β), phospho-GSK3α/β (S21/9), MEK1/2, phospho-MEK1/2 (S217/221), mechanistic target of rapamycin (mTOR), phospho-mTOR (S2448), 90 kDa ribosomal S6 kinase 1/2/3 (RSK1/2/3), phospho-p90RSK (S380), Src, phospho-Src (Y416), myeloid cell leukemia sequence 1 protein (MCL-1), β-catenin, E-cadherin, and vimentin. Blots were incubated with horseradish peroxidase–conjugated secondary antibodies (1:15,000; Santa Cruz) and immunoreactive protein bands were visualized by the enhanced chemiluminescence system (PerkinElmer). The membrane was then stripped and re-probed with β-actin (1:4000, Sigma-Aldrich) as a loading control. Band areas of individual proteins were quantified using the ImageJ software (https://imagej.nih.gov/ij/). Normalization for loading differences was achieved by dividing the densitometry values for individual proteins by the densitometry values for β-actin in the same lane. Protein expression levels in the drug-treated tumors were expressed as relative to those in the control tumors. For phosphorylated proteins, the signal values were expressed as the ratio of phosphorylated to total species relative to that of the control tumors.

Quantitative Determination of Dasatinib and Sorafenib Concentrations in Plasma and Tumors

A HPLC method was developed and validated for simultaneous determination of dasatinib and sorafenib in mouse plasma and xenograft tumor tissues. Plasma and

JPET Fast Forward. Published on October 11, 2017 as DOI: 10.1124/jpet.117.240507
This article has not been copyedited and formatted. The final version may differ from this version.

tumor tissue homogenate (tissue:MilliQ water = 1: 9, w/v) samples were deproteinated by adding three volumes of methanol containing 5 μg/mL of 7-hydroxywarfarin (the internal standard, IS) followed by the centrifugation at 13,000 rpm for 10 minutes. Ten microliter aliquots of the supernatants were injected onto the reversed-phase HPLC system with a diode array detector. The chromatographic separation was achieved on an octadecylsilane bonded silica column (Luna® 3μm C18, 50 × 4.6 mm, Phenomenex) at room temperature. Gradient elution was employed using 20% acetonitrile containing 10 mM ammonium acetate and 0.1% formic acid as solvent A and 60% acetonitrile containing 10 mM ammonium acetate and 0.1% formic acid as solvent B, with a linear gradient increasing from 0 to 100% B from 1 to 3 min, maintaining 100% B from 3 to 9 min, decreasing from 100 to 0% B from 9 to 11 min. The total run time was 14 min. Dasatinib and IS were best detected at 325 nm, and sorafenib was best detected at 255 nm. Retention time was about 5.8, 6.7 and 8.4 min for dasatinib, IS and sorafenib, respectively. Standard curves of dasatinib and sorafenib were linear within the ranges of 62 – 5000 ng/ml ($r^2 > 0.99$) in plasma and tumor homogenates, respectively. The lower limits of quantitation (LLOQ) in plasma and tumor tissue homogenates were 62 ng/ml for both dasatinib and sorafenib.

Statistical Analyses

Statistical analyses were performed using Number Cruncher Statistical Systems 2007 (Keysville, UT). Data are presented as the mean ± standard deviation (SD) unless otherwise indicated. Comparison of means from two matched groups was made using the paired-sample *t* test. Comparison of means between two independent groups was made using the independent sample *t* test. In case of multiple comparisons, Kruskal-

Wallis one-way analysis of variance on ranks followed by the post-hoc Kruskal-Wallis multiple comparison z-value test was used. Pearson correlations were used to describe relations between two variables. A two-sided *P*-value of less than 0.05 was considered statistically significant.

Results

In Vivo Selection of Sorafenib-Resistant A549 Xenograft Line

Given that patients with *EGFR*-wild-type and *KRAS*-mutant NSCLC have been shown to benefit from sorafenib treatment in recent clinical trials (Blumenschein et al., 2013; Dingemans et al., 2013), the A549 human adenocarcinoma cell line expressing wild-type *EGFR* and harboring a G12S *KRAS* mutation (Mahoney et al., 2009) was used to establish the *in vivo* sorafenib resistant tumor model. It has been reported that treatment with 30 to 60 mg/kg of sorafenib led to complete tumor stasis in the A549 xenograft (Wilhelm et al., 2004). Therefore, in this study, A549 tumor bearing athymic nude mice were given oral administration of 40 mg/kg/d of sorafenib. The treatment was well tolerated by the animals. No deaths nor obvious side effects were observed. At such dose level, a highly statistically significant inhibition of tumor growth corresponding to a mean tumor size reduction of up to 86% was observed. Mice in the control group reached the predetermined endpoint (tumor volume = 1000 mm^3) earlier and thus were on study for a shorter period of time than were the sorafenib-treated mice (6 weeks for mice in the control group versus 15 weeks for those in the sorafenib-treated group, Fig. 1A). During the 15-week treatment period, sorafenib-treated mice exhibited different tumor growth rates. The fold change of tumor volume (i.e., the tumor growth index

value) after the 15-week treatment period ranged from 0.9 – 30.2 with the median value of 3.6 (Fig 1B). The fastest growing sorafenib-treated A549 xenograft with a tumor growth index value of 30.2 was used to derive the A549/SRFres subclone for the subsequent study. Further evaluation of the A549/SRFres xenograft model in comparison with the A549 xenograft model was conducted in individual mice receiving simultaneous subcutaneous inoculations of A549 cells on the left flank and A549/SRFres cells on the right flank (Fig. 1C). Two of the vehicle-treated animals and two of the sorafenib-treated animals were euthanized after 8 weeks of treatment, and one vehicle-treated animal was euthanized after 10 weeks of treatment, due to their tumors reaching the maximum allowed volume (i.e., 1000 mm^3). One time-matched sorafenib-treated animal was euthanized after 10 weeks of treatment. There was no significant difference in tumor volume among all study groups when the treatment was initiated one week after tumor inoculation (Supplemental Figure S1). Significant suppression of tumor growth by sorafenib treatment was observed from Weeks 9 to 12 ($P < 0.05$ for both A549 and A549/SRFres tumors as compared with the corresponding vehicle control. Fig.1D). A549/SRFres tumors exhibited relatively rapid tumor growth rates as compared with A549 tumors during the 12-week treatment period. For the vehicle control group, the difference in tumor volume between A549 and A549/SRFres tumors was statistically significant at Week 2, 3, 4, 5, 6 and 12 ($P < 0.05$, Fig. 1D). For the sorafenib treatment group, the significant difference in tumor volume between A549/SRFres tumors and their parental counterparts was observed at Week 2, 3, 5, 6, 9, 10 and 11 ($P < 0.05$. Fig. 1D). The mean tumor growth index value for the A549/SRFres xenografts was higher than that for the A549 xenografts (13.7 $\pm$ 3.9

JPET Fast Forward. Published on October 11, 2017 as DOI: 10.1124/jpet.117.240507
This article has not been copyedited and formatted. The final version may differ from this version.

versus 8.7 ± 5.3), but the difference was not statistically significant (P = 0.184). In terms of tumor response to sorafenib treatment, sorafenib effectively suppressed the growth of both A549 and A549/SRFres xenografts as demonstrated by the 67% (P < 0.05) and 56% (P < 0.01) decrease in the mean tumor growth index values for A549 and A549/SRFres tumors, respectively. A comparison of tumor growth rate between the sorafenib-treated A549/SRFres tumors and their parental counterparts showed that the mean volumes of A549/SRFres tumors were significantly larger than those of the A549 tumors at Weeks 3, 4 and 6 after the start of the treatment (P < 0.05). Moreover, the mean tumor growth index value for the sorafenib-treated A549/SRFres tumors was significantly higher than that of the A549 tumors (6.0 ± 3.9 versus 2.9 ± 1.3, P < 0.05). These results suggest that the A549/SRFres tumors display relatively higher resistance to sorafenib than their parental counterparts. Taken together, sorafenib-treated A549/SRFres tumors demonstrated significantly rapid growth as compared with their sorafenib-treated parental counterparts, which may be in part attributable to the relatively rapid baseline A549/SRFres tumor growth.

Identification of Potential Mechanisms Associated with Acquired Sorafenib Resistance

To identify molecular mechanisms involved in the acquired sorafenib resistance, Western blot analysis was performed to assess the levels of selected EMT markers and protein kinases in vehicle- and sorafenib-treated A549 and A549/SRFres tumors (Fig. 2). For the A549 xenografts, a significant decrease in the β-catenin expression level was found in sorafenib-treated tumors as compared with the control tumors (44% decrease, P < 0.05. Fig. 2B). With regard to the A549/SRFres xenografts, both β-

catenin and E-cadherin expression levels were significantly decreased (36% decrease and $P < 0.05$ for both), while the MMP9 (362% increase, $P < 0.01$) and phospho-FAK (138% increase, $P < 0.05$. Fig. 2B) levels were significantly increased in the sorafenib-treated tumors as compared with those in the control tumors. It was also noted that there were 56% and 59% increase in the expression of phospho-Src in the A549 and A549/SRFres tumors, respectively, although the statistical significance was not reached ($P = 0.099$ and 0.069 for A549 and A549/SRFres tumors, respectively). Nonetheless, given the prominent role of Src in the receptor tyrosine kinase (RTK)-mediated signal transduction through the activation of RAS/RAF/MAPK and PI3K/AKT pathways that promotes cell survival, mitogenesis, and migration and invasion (Bromann et al., 2004; Thamilselvan et al., 2007), this finding prompted us to speculate that activation of FAK-Src signaling pathway creates a bypass track that promotes resistance to sorafenib, and the use of a Src inhibitor in combination with sorafenib may antagonize sorafenib resistance conferred by the FAK-Src-mediated bypass signaling pathway.

No Changes in Proliferation and Migratory and Invasive Phenotype in A549/SRFres Cells in Comparison with A549 Parental Cells *in Vitro*

To examine the impact of long-term *in vivo* therapeutic pressure imposed by sorafenib on the *in vitro* behavior of A549/SRFres cells, measurement of doubling time, wound-healing assay and transwell invasion assay were conducted. No significant difference in doubling time was found between A549 parental and A549/SRFres cells (23.7 ± 1.9 hr versus 24.3 ± 1.7 hr, $P > 0.05$). Moreover, the migratory (Fig. 3A) and invasive (Fig. 3B) phenotype of A549/SRFres cells appeared to be similar to that of A549 cells ($P > 0.05$

for all). These data suggest that the aggressive behavior of A549/SRFres cells acquired *in vivo* under the therapeutic pressure is reversible.

Examination of Molecular Changes Induced by Sorafenib and Dasatinib Treatment in Cultured A549 and A549/SRFres Cells

To confirm if the activation of FAK-Src signaling pathway was responsible for the acquired sorafenib-resistance phenotype in A549 xenograft tumors, the baseline and treatment-induced changes in protein expression levels of EMT markers and downstream signaling molecules regulating cell proliferation, migration and invasion, were compared between A549 parental and A549/SRFres cells. As shown in Fig. 3C, the baseline expression levels of phospho-Src (Y416) and phospho-FAK (Y576/577) were markedly increased by 60% and 110%, respectively, in A549/SRFres cells as compared with those in A549 parental cells. Treatment with 10 μM of sorafenib for 4 hours had no effect on the expression of phospho-Src and phospho-FAK (Y576/577). In contrast, dasatinib treatment at 0.02 and 0.2 μM was sufficient to inhibit the phosphorylation of Src at Tyr-416 and FAK at Tyr-576/577. Moreover, the combined sorafenib and dasatinib treatment appeared to result in a greater degree of decrease in Src phosphorylation in A549/SRFres cells than it did in A549 cells, suggesting that A549/SRFres cells with elevated phospho-Src levels is relatively sensitive to the sorafenib-dasatinib combination treatment. No notable difference was found in either baseline expression levels or treatment-induced changes in the expression levels of other proteins evaluated between A549 parental and A549/SRFres cells.

JPET Fast Forward. Published on October 11, 2017 as DOI: 10.1124/jpet.117.240507
This article has not been copyedited and formatted. The final version may differ from this version.

In Vitro Evaluation of Cytotoxic Effect of Sorafenib-Dasatinib Combination in A549 Parental and A549/SRFres cells

To evaluate the *in vitro* cytotoxic effect of the combination treatment with sorafenib and dasatinib in A549 and A549/SRFres cells, sorafenib and dasatinib were used at the fixed molar ratios of 1:3, 1:1 and 3:1. Quantitative analyses of the dose-effect relationships of sorafenib and dasatinib treatment alone and in combination showed that the IC_{50} values for sorafenib and dasatinib alone in the A549 cell line were similar to those in its sorafenib-resistant subclone (i.e., A549/SRFres), while the combined sorafenib and dasatinib treatment resulted in a greater inhibitory effect on cell proliferation than treatment with either drug alone in both cell lines (Fig. 4A). In applying the combination index (CI) method to the data in Fig. 4A, we assume that sorafenib and dasatinib were mutually nonexclusive, *i.e*. the action of sorafenib on RAF/VEGFR /PDGFR did not affect the action of dasatinib on Src/ABL. For A549/SRFres cells, simultaneous and continuous exposure to sorafenib and dasatinib at the fixed molar ratios of 1:1 and 3:1 for 72 h showed synergism (CI < 1) for fraction affected (FA) values between 0.1 and 0.9, while the combination of sorafenib and dasatinib at the fixed molar ratio of 1:3 showed synergism (CI < 1) when FA values were greater than 0.4. For A549 cells, simultaneous exposure to sorafenib and dasatinib at the molar ratio of 1:1 produced an additive to weak synergistic effect for FA values ranging from 0.2 to 0.8, which sorafenib and dasatinib at the molar ratio of 1:3 and 3:1 resulted in an additive to synergistic effect for FA values greater than 0.4 (Fig. 4B, Supplemental Table S1). Taken together, these data clearly indicate that combination treatment with sorafenib

and dasatinib is effective against A549 and A549/SRFres cells when used at a molar concentration ratio between 1:3 and 3:1.

In Vivo Response of A549 and A549/SRFres Xenograft Models to Sorafenib and Dasatinib Alone and in Combination

Since we observed the additive and synergistic cytotoxic effects of concurrent treatment with sorafenib and dasatinib on A549 and A549/SRFres cells *in vitro*, we next evaluated the antitumor effect of individual and combination treatments with sorafenib and dasatinib on the established A549 and A549/SRFres lung cancer xenografts. No significant difference in tumor volume was observed among all study groups when the treatment was initiated three weeks after tumor inoculation (Supplemental Figure S2 and S3). Sorafenib and dasatinib monotherapies at the dose level of 20 mg/kg/d significantly suppressed the growth of A549/SRFres xenografts with the maximum percent tumor growth inhibition of 45% ($P < 0.01$) and 35% ($P < 0.05$), respectively, but were unable to significantly inhibit the growth of A549 tumors (Supplemental Figure S3). As shown in Fig. 4C, in A549 xenografts, the effect of 40 mg/kg/d sorafenib on tumor growth arrest became significant 1.5 weeks after the start of the treatment with the maximum percent tumor growth inhibition of 72% ($P < 0.01$ compared with the control). Tumor growth inhibition did not become significant until 3.5 weeks after the start of the sorafenib-dasatinib combination treatment with the maximum percent tumor growth inhibition of 53% ($P < 0.05$. Fig. 4C). Only 30% maximum tumor growth inhibition was achieved with 40 mg/kg/d dasatinib treatment alone ($P > 0.05$. Fig. 4C). In A549/SRFres xenografts, the inhibitory effect of sorafenib alone and half-dose combination of sorafenib and dasatinib on tumor growth became significant one week after the start of

the treatment with the maximum percent tumor growth inhibition of 75% and 69%, respectively ($P < 0.01$ compared with controls for both. Fig.4D). In contrast, although dasatinib monotherapy was able to produce a maximum percent tumor growth inhibition of 52% ($P > 0.05$ compared with the control. Fig. 4D), the inhibitory effect of dasatinib on tumor growth was not statistically significant except for Week 3 ($P < 0.05$. Fig. 4D). When compared with the parental counterparts, vehicle- and sorafenib-treated A549/SRFres tumors demonstrated significantly higher tumor growth rate ($P < 0.05$ or $P < 0.01$ using paired sample t test. Fig. 4D). However, the tumor growth rates dasatinib- and combination-treated A549/SRFres tumors were not significantly different from those of their corresponding parental counterparts ($P > 0.05$. Fig. 4D). Overall, in both A549 and A549/SRFres xenografts, treatment with sorafenib alone at 40 mg/kg/d resulted in the most significant tumor growth inhibition, which was significantly more than what was achieved by treatment with 40 mg/kg/d of dasatinib. The half-dose sorafenib-dasatinib combination was more effective than the 20 mg/kg/d dasatinib monotherapy in both A549 ($P < 0.05$) and A549/SRFres ($P < 0.01$) xenografts, and also more effective than the 20 mg/kg/d sorafenib treatment in A549/SRFres xenografts ($P < 0.05$. Supplemental Figure S4). No significant difference in mean tumor volumes was observed between the 40 mg/kg/d sorafenib monotherapy and half-dose sorafenib-dasatinib combination groups in either A549 or A549/SRFres xenografts ($P > 0.05$. Fig. 4C and 4D). Moreover, significantly rapid tumor growth was observed in vehicle- and sorafenib-treated A549/SRFres tumors, but not in dasatinib- and combination-treated A549/SRFres tumors, as compared with their corresponding parental counterparts.

Effects of Sorafenib and Dasatinib Alone and in Combination on Tumor Angiogenesis, Tumor Cell Proliferation and Adhesion in A549 and A549/SRFres Xenografts

Results of immunofluorescence staining of cultured A549 and A549/SRFres cells demonstrated that there was no difference in baseline Ki67, E-cadherin, α-SMA and collagen IV expression levels between those two cell lines (Supplemental Figure S5). Nonetheless, the observed tumor growth inhibition following treatment with full-dose sorafenib and half-dose sorafenib-dasatinib combination in the A549 and A549/SRFres xenograft models warranted further assessment of the mechanisms underlying the *in vivo* anti-tumor activities of individual and combination treatments. Proliferation is a key feature of tumor progression and is often estimated by the immunohistochemical assessment of the nuclear antigen Ki67. Results from this study demonstrated a decrease in the mean Ki67 proliferative index values following the full-dose sorafenib and half-dose combination therapies in both A549 and A549/SRFres xenografts although only the decrease in A549/SRFres tumors was statistically significant compared with the control tumors ($P < 0.05$ for both full-dose sorafenib and half-dose combination therapies, Fig.5A and 5B). Nonetheless, the mean Ki67 proliferative index value in sorafenib-treated A549/SRFres tumors was significantly increased compared with that in their parental counterparts (by 38%, $P < 0.05$), suggesting an attenuated sorafenib antiproliferative activity in A549/SRFres tumors (Fig. 5B). In addition, the Ki-67 proliferative index values were highly correlated with the volumes of both A549 and A549/SRFres tumors at Week 4 (Pearson: $r = 0.544$ for A549, $r = 0.542$ for A549/SRFres, $N = 28$ and $P < 0.01$ for both), suggesting that inhibitory effect of

JPET Fast Forward. Published on October 11, 2017 as DOI: 10.1124/jpet.117.240507
This article has not been copyedited and formatted. The final version may differ from this version.

sorafenib and dasatinib on tumor growth is attributable to the anti-proliferative activities of individual drugs. In addition, the results of Ki-67 immunofluorescence staining were in line with the results of the H&E staining of tumor sections, which revealed that relatively large regions of necrosis were present in tumors receiving drug treatments as compared with the control tumors (Supplemental Figure S6).

E-cadherin plays a crucial role in maintaining cell-cell adhesion in epithelial tissues. Downregulation of E-cadherin expression is associated with tumor progression, invasion and metastasis (Rodriguez et al., 2012). Results of the immunofluorescence staining of tumor sections showed that E-cadherin expression levels were significantly reduced in sorafenib-treated A549 tumors (decreased by 30%, $P < 0.05$) but not in sorafenib treated A549/SRFres tumors (decreased by 8%, $P > 0.05$) as compared with the corresponding controls (Fig. 5C).

Effects of individual and combination treatments on tumor vasculature were evaluated using the immunohistochemical markers for endothelial cells (with CD31), microvessel basement membrane (with collagen-IV) and mural cells, *i.e*. pericytes and smooth muscle cells (with α-SMA) (Fig. 5A, 5D-5F). As a potent antiangiogenic agent, sorafenib was able to reduce the microvessel density (MVD) determined by the CD31 positive staining in both A549 ($P < 0.01$) and A549/SRFres ($P < 0.05$) xenografts, while full-dose dasatinib treatment resulted in a significant decrease in MVD in A549 xenografts ($P < 0.05$), but not in A549/SRFres xenografts. Notably, the mean MVD in dasatinib-treated A549/SRFres tumors was significantly higher than that in their parental counterparts ($P < 0.05$), suggesting dasatinib has no effect on tumor angiogenesis in A549/SRFres tumors. A significant decrease in MVD following the half-dose sorafenib-dasatinib

JPET Fast Forward. Published on October 11, 2017 as DOI: 10.1124/jpet.117.240507
This article has not been copyedited and formatted. The final version may differ from this version.

combination therapy was seen in A549/SRFres tumors ($P < 0.05$) but not A549 tumors (Fig. 5D). With regard to collagen-IV, full-dose sorafenib treatment significantly reduced collagen-IV expression levels in A549 tumors but not in A549/SRFres tumors as compared with the vehicle control and half-dose sorafenib-dasatinib combination ($P < 0.05$ for both). Full-dose dasatinib treatment significantly increased collagen-IV expression in A549/SRFres tumors compared with that in their parental counterparts ($P < 0.05$), which was consistent with its diminished effect on MVD in A549/SRFres tumors. Compared with full-dose dasatinib treatment, the half-dose combination therapy was able to lower the collagen-IV expression levels in A549/SRFres tumors significantly ($P < 0.05$) (Fig. 5E). As for α-SMA, no statistically significant difference was found among the study groups, suggesting none of the treatments affect mural cells in the tumor (Fig. 5F). Taken together, results of the immunofluorescence staining of tumor tissues confirmed that the antitumor effect of sorafenib and dasatinib was attributable to their antiproliferative and antiangiogenic properties, and A549/SRFres tumors exhibited a relatively higher cell proliferation rate than A549 tumors.

Mechanisms Underlying the Anti-Tumor Effects of Sorafenib and Dasatinib Alone and in Combination in A549 and A549/SRFres Xenografts

In addition to the histological analyses, Western blot analysis was carried out to elucidate the molecular events underpinning the tumor growth inhibition mediated by sorafenib and dasatinib alone and in combination and identify any potential escape routes developed during the treatment (Supplemental Figure S7 and S8). In A549 xenografts, compared with the control tumors, the 40 mg/kg/d sorafenib treatment significantly decreased the expression of MCL-1 (by 38%, $P < 0.01$) and phospho-

GSK3α (by 55%, P < 0.01), but increased the expression of phospho-AKT (by 30%, P < 0.05). The 40 mg/kg/d dasatinib treatment, on the other hand, significantly decreased the expression of phospho-Src (by 50%, P < 0.05) and phospho-ERK (by 19%, P < 0.05), but increased the Y397-FAK phosphorylation (by 191%, P < 0.05). Half-dose sorafenib-dasatinib combination resulted in a significant decrease in the expression of phospho-ERK (by 21%, P < 0.05), and a significant increase in the Y397-FAK phosphorylation (by 119%, P < 0.05). In addition, the expression of phospho-Src in 40 mg/kg/d dasatinib-treated A549 tumors was 58% lower than that in sorafenib-treated A549 tumors (P < 0.05), while the phospho-AKT expression in A549 tumors treated with the half-dose combination was 26% lower than that in sorafenib-treated A549 tumors (P < 0.05) (Fig. 6A). In similar fashion, 20 mg/kg/d sorafenib treatment significantly reduced the phosphorylation of GSK3α (P < 0.05), while 20 mg/kg/d dasatinib treatment resulted in significant decrease in Y416-Src phosphorylation and Y576/577-FAK phosphorylation (P < 0.05 and P < 0.01 compared with the vehicle and 20 mg/kg/d sorafenib treatment, respectively. Supplemental Figure S8A). In A549/SRFres tumors, as compared with the control tumors, 40 mg/kg/d sorafenib significantly decreased the expression of MCL-1 and phospho-GSK3α by 16% and 53%, respectively (P < 0.05 for both), but increased the phospho-Src expression by 114% (P < 0.05). Dasatinib treatment at 40 mg/kg/d significantly reduced the expression of phospho-GSK3α and phospho-MEK by 38% (P < 0.05) and 21% (P < 0.01), respectively, but increased the Y397-FAK phosphorylation by 177% (P < 0.05) as compared with the control. Moreover, the half-dose combination therapy significantly decreased the expression of MCL-1 and phospho-GSK3α by 17% and 38% (P < 0.05 for both), respectively, while the Y397-FAK

phosphorylation was increased by 192% ($P < 0.01$) as compared with the control. Furthermore, the expression of phospho-Src in 40 mg/kg/d sorafenib-treated A549/SRFres tumors was significantly increased as compared with that in A549/SRFres tumors treated with 40 mg/kg/d dasatinib alone (by 95%, $P < 0.01$) and the combination of sorafenib and dasatinib (by 71%, $P < 0.05$), suggesting dasatinib effectively inhibits Src activation in the tumor. In addition, the phospho-AKT expression level in the half-dose combination group was lower than that in the full-dose dasatinib group (by 17%, $P < 0.05$) (Fig. 6C). Similarly, 20 mg/kg/d sorafenib and dasatinib monotherapies significantly decreased the expression of phospho-GSK3α ($P < 0.05$ for both). The expression of phospho-Src ($P < 0.05$), pAKT ($P < 0.05$) and phospho-p90RSK ($P < 0.01$) in 20 mg/kg/d dasatinib-treated A549/SRFres tumors was significantly reduced as compared with that in 20 mg/kg/d sorafenib treated tumors (Supplemental Figure S8C). Results of the paired-sample t test comparing between the matched A549 and A549/SRFres tumor samples indicated that the phospho-ERK and phospho-GSK3β levels were significantly decreased in the sorafenib-treated and sorafenib-dasatinib-treated A549/SRFres tumors, suggesting ERK and GSK3β are unlikely involved in the bypass mechanism of sorafenib resistance (Fig. 6E). Taken together, although dasatinib alone or in combination with sorafenib significantly reduced the phospho-Src levels in A549 and A549/SRF tumors as compared with those in the sorafenib-treated tumors, the phospho-FAK (Y397) levels remained elevated in all treatment groups regardless of tumor types. In terms of other downstream effectors involved in the antitumor effect of sorafenib, including MCL-1, phospho-AKT, phospho-ERK, phospho-MEK, phospho-p90RSK, phospho-GSK-3α/β (Liu et al., 2006; Ulivi et al., 2009), the inhibitory effect of

half-dose sorafenib-dasatinib combination on the expression levels of those proteins was comparable to the full-dose sorafenib or dasatinib treatment regardless of tumor types.

Several lines of evidence have suggested that sorafenib resistance is associated with the activated EMT process and increased tumor metastatic potential (Wang et al., 2014). Therefore, we examined the effects of single agent and combination treatment on the biomarkers of EMT, including E-cadherin, β-catenin and vimentin, and the selected biomarkers of tumor metastatic potential, including MMP9 and α-SMA, in the A549 and A549/SRFres xenograft model (Supplemental Figure S7 and S8, Fig. 6B, 6D and 6F). In both A549 and A549/SRFres tumors, the full-dose sorafenib treatment led to a significant decrease in the expression of epithelial cell marker E-cadherin (by 44% and $P < 0.01$ for A549, and by 38% and $P < 0.05$ for A549/SRFres) and a significant increase in the expression of mesenchymal cell marker vimentin (by 25% and $P < 0.05$ for A549, and by 45% and $P < 0.05$ for A549/SRFres) as compared with the control. Also, the expression of vimentin was significantly increased in A549 (by 20%) and A549/SRFres (by 39%) tumors treated with the half-dose sorafenib-dasatinib combination as compared with the control tumors ($P < 0.05$ for both). The full-dose dasatinib treatment resulted in a significant increase in MMP9 expression in A549 (by 268%) and A549/SRFres (by 177%) tumors as compared with the vehicle control ($P < 0.01$ for both), while the MMP9 expression levels were significantly increased in A549/SRFres tumors treated with half-dose sorafenib-dasatinib combination (by 233% and $P< 0.05$ compared with the control) (Fig. 6B and 6D). Sorafenib treatment at the dose of 20 mg/kg resulted in a significantly decreased β-catenin expression in A549

tumors ($P < 0.05$), while both 20 mg/kg/d sorafenib and dasatinib monotherapies increased the expression of vimentin in A549/SRFres tumors ($P < 0.05$ for both. Supplemental Figure S8B and S8D). In addition, the expression levels of E-cadherin and α-SMA in the full-dose dasatinib-treated A549 tumors were significantly higher than those in the full-dose sorafenib-treated A549 tumors ($P < 0.05$ for E-cadherin and $P < 0.01$ for α-SMA) (Fig. 6B). Comparison between matched A549 and A549/SRFres tumors indicated that the E-cadherin level was significantly decreased in 40 mg/kg/d sorafenib-treated A549/SRFres tumors, suggesting that A549/SRFres tumor cells are more susceptible to EMT under the therapeutic pressure imposed by sorafenib *in vivo*. Moreover, the MMP9 level in 20 mg/kg/d sorafenib- and 40 mg/kg/d dasatinib-treated A549/SRFres tumors was significantly lower than that in their parental counterparts, implicating that dasatinib is relatively more effective at inhibiting the progression of A549/SRFres tumors compared with that of A549 tumors (Fig. 6F and Supplemental Figure 8F). Taken together, these findings suggest that sorafenib treatment promotes EMT in A549 xenografts, and the presence of dasatinib does not suppress the sorafenib-induced EMT but may increase the metastatic potential as demonstrated by the increased MMP9 and α-SMA expression levels in tumors.

There were discrepancies between the two *in vivo* studies regarding the expression levels of individual EMT markers in sorafenib-treated tumors relative to those in the control tumors. For example, although sorafenib treatment resulted in significant downregulation of β-catenin and modest upregulation of vimentin in both A549 and A549/SRFres tumors in the initial study, the second *in vivo* study showed little change in β-catenin expression but significant upregulation of vimentin in sorafenib-treated tumors

as compared with the control tumors. Those discrepancies may be explained partly by the difference in time to initiate treatment (one week versus three weeks following tumor inoculation) and treatment duration (8~12 weeks versus 4 weeks)

Evaluation of Sorafenib and Dasatinib Steady State Concentrations in Plasma and Tumors

Concentrations of sorafenib and dasatinib in plasma and tumors collected at 4 hours after the last dose were quantified to determine if the reduced effectiveness was attributable to decreased drug distribution in sorafenib-resistant tumors and if there was any pharmacokinetic drug-drug interaction in which one drug altered the tumor distribution of the other co-administered drug. As shown in Table 1, there was no significant difference in steady-state tumor concentrations of sorafenib and dasatinib between A549 and A549/SRFres xenografts. Both sorafenib and dasatinib exhibited dose proportional changes in plasma and tumor drug concentrations at 4 hours after the last dose, suggesting linear pharmacokinetics. Dasatinib plasma concentrations were lower than sorafenib plasma concentrations when these two drugs were given at the same dose, suggesting that dasatinib has a shorter elimination half-life than sorafenib. As a result, dasatinib tumor concentrations at 4 hours were about 1.7-fold lower than sorafenib tumor concentrations irrespective of tumor types (Table 1).

Discussion

Although considerable efforts have been made to investigate mechanisms underpinning the acquired sorafenib resistance in various types of cancer, none has focused on NSCLC. In this study, an A549 human lung adenocarcinoma xenograft model was used

to explore the potential mechanism of acquired sorafenib resistance. *In vivo* drug resistant models are more advantageous than *in vitro* models because they provide the tissue microenvironment in which tumor cells reside. The model used in this study was established using a sorafenib-resistant A549 subline derived from the fastest growing A549 tumor that has become insensitive to sorafenib treatment *in vivo*. Comparing with serial *in vivo* passaging of primary tumors, using the sorafenib-resistant A549 subline with low passage numbers (< 10) has the advantage of providing reproducible insights into the biologically relevant mechanism underlying the resistance and facilitating the process of identifying effective therapeutic strategy to overcome the resistance, yet suffers the drawback of possible changes in certain genetic features of primary tumors during the *in-vivo-to-in-vitro-to-in-vivo* transition. An intriguing observation of our *in vivo* study was that A549/SRFres xenografts exhibited significantly rapid growth compared with their corresponding parental counterparts (Fig. 1D and 4D), even though the doubling time of cultured A549/SRFres cells was similar to that of A549 cells. This finding raises the possibility that the prior selection process enables A549/SRFres cells to acquire certain traits that allow them to adapt to the microenvironmental proliferation barriers more quickly than A549 parental cells. Despite the differential tumor growth rate observed *in vivo*, we were able to use this model to identify a new bypass mechanism of acquired sorafenib resistance and evaluate if dasatinib can be a potential adjunct to sorafenib therapy to overcome the resistance.

Examination of the expression pattern of several EMT markers in A549 and A549/SRFres xenografts revealed the tendency of downregulated E-cadherin and upregulated vimentin expression in sorafenib-treated tumors as compared with the

controls (Fig. 2B, 6B and 6C). Sorafenib-treated A549/SRFres xenografts appeared to undergo similar EMT event as the sorafenib-treated A549 xenografts but to a greater extent (Fig. 6F). EMT, which activation often results in aggressive tumor behaviors, has been associated with resistance to sorafenib in hepatocellular carcinoma (HCC) models. In a recent study, the *in-vitro* established sorafenib-resistant HepG2 and Hus7S1 cell lines displayed a loss of E-cadherin and an increase in vimentin expression, which was accompanied by an increased invasive potential (van Malenstein et al., 2013). In this study, no marked difference in the expression of selected EMT markers was observed between cultured A549 and A549/SRFres cells, nor was any difference found in their migratory and invasive phenotype irrespective of the treatment (Fig. 3), suggesting the crucial role of tumor microenvironment in inducing the EMT (Jing et al., 2011). The exact mechanism accounting for the significant decrease in β-catenin levels in both sorafenib-treated A549 and A549/SRFres tumors is unclear. Nonetheless, it has been reported that loss or downregulation of β-catenin was associated with disease progress in malignant melanoma (Kageshita et al., 2001), and sorafenib was effective in decreasing β-catenin protein levels in human liver cancer cell lines (Lachenmayer et al., 2012). Therefore, we speculate that the decreased β-catenin levels in tumor tissue homogenates might be due to the decreased membranous and cytoplasmic β-catenin levels as a result of the loss of interaction between E-cadherin and β-catenin that potentially releases β-catenin from cell adherens junctions (Onder et al., 2008) followed by the nuclear translocation of β-catenin leading to the induction of EMT (Alvarado et al., 2011; Ghahhari and Babashah, 2015).

In this study, besides the significant upregulation of MMP9 protein expression in sorafenib-treated A549/SRFres tumors, we also observed the elevated expression levels of phospho-AKT (S473), phospho-FAK (Y397) and phospho-Src (Y416) in 40 mg/kg/d sorafenib-treated A549 and A549/SRFres tumors with no statistical significance in part due to the large interindividual variability. Nonetheless, our *in vitro* study demonstrated that the baseline phospho-Src (Y416) and phospho-FAK (Y576/577) levels in A549/SRFres cells were markedly higher than those in A549 cells (Fig. 3C). Given that activation of FAK and AKT signaling pathways has been suggested to upregulate the MMP9 expression in HCC leading to the enhanced cell invasion (Cheng et al., 2006; Chen et al., 2010a), it is tempting to speculate that AKT, FAK and Src are potential alternate signaling molecules being activated to evade sorafenib therapy. Compensatory activation of the PI3K/AKT signaling pathway has been reported to mediate acquired sorafenib resistance (Chen et al., 2011), and therapeutic synergy could be achieved by combining sorafenib with PI3K/AKT inhibitors (Chen et al., 2010b; Zhai et al., 2015; Lindblad et al., 2016). In addition, activation of PI3K/AKT pathway downregulates membranous E-cadherin and β-catenin levels and promotes tumor cell invasion (Yip and Seow, 2012), suggesting the observed downregulation of E-cadherin and β-catenin in sorafenib-treated tumors may attribute to sorafenib-induced activation of PI3K/AKT pathway. Although sorafenib-induced activation of FAK and Src has not been documented so far, the possible connection between FAK and acquired sorafenib resistance has been described in a recent study, which showed that the αvβ3-integrin/FAK/PI3K/AKT signaling pathway was involved in galectin-1 induced EMT and sorafenib resistance in HCC cells (Zhang et al., 2016). FAK and Src are cytoplasmic

nonreceptor tyrosine kinases influencing cell adhesion by their direct or indirect effects on other adhesion regulators (Calautti et al., 1998; Noren et al., 2001). FAK is a downstream target of several growth factors (Mitra et al., 2005), while Src is a crucial mediator of FAK-regulated processes (Westhoff et al., 2004). The FAK-Src complex is activated through integrin-stimulated FAK phosphorylation at Y397, which creates a binding site for Src. Src in turn mediates the phosphorylation of Y576/Y577 in the FAK domain activation loop, which subsequently activates the p130Cas-associated motility-promoting signaling cascades, leading to the induction and activation of MMP2 and MMP9 that promote cancer cell invasion (Van Slambrouck et al., 2007).

Based on our initial findings, we proposed an alternative survival mechanism that would allow the *KRAS*-mutant NSCLC to escape from sorafenib therapy through the activation of FAK/Src complex. Given the essential role of Src in mediating FAK phosphorylation and driving tumor cell proliferation, survival, adhesion, motility and invasion (Bromann et al., 2004; Thomas and Jordan, 2004), we next examined if sorafenib in combination with dasatinib could increase antitumor efficacy and delay the onset of acquired sorafenib resistance. Results of the *in vitro* study showed that simultaneous exposure to sorafenib and dasatinib at fixed molar ratios of 3:1, 1:1 and 1:3 produced mostly additive to synergistic cytotoxic effects in both A549 and A549/SRFres cells, suggesting that simultaneous administration of sorafenib and dasatinib is an appropriate schedule for this combination. Determination of sorafenib and dasatinib concentrations in plasma and tumors demonstrated that the intratumoral concentration ratio of sorafenib to dasatinib was about 3, which was within the range of concentration ratio that had produced synergistic effect *in vitro*. In agreement with the *in vitro* data (Fig. 4A-4B), it

JPET Fast Forward. Published on October 11, 2017 as DOI: 10.1124/jpet.117.240507
This article has not been copyedited and formatted. The final version may differ from this version.

appeared that dasatinib alone or in combination with sorafenib resulted in a relatively greater tumor growth inhibition in A549/SRFres tumors than that in A549 tumors (Fig. 4C-4D). The augmented susceptibility of A549/SRFres tumors to dasatinib treatment may be associated with the upregulated baseline FAK-Src activity in A549/SRFres cells (Fig. 3C). Despise the evidence of *in vitro* synergy between sorafenib and dasatinib, the *in-vivo* anti-tumor effect of half-dose sorafenib-dasatinib combination therapy was inferior to that of the full-dose sorafenib treatment but superior to that of the full-dose dasatinib treatment regardless of tumor types. Nonetheless, the half-dose sorafenib-dasatinib combination exhibited a greater anti-tumor activity than single-agent sorafenib or dasatinib when used at the same dose. As indicated by the Western blotting analysis, although the half-dose combination effectively inhibited Src and AKT phosphorylation, it did not block Y576/577-FAK phosphorylation nor decrease vimentin expression in tumors, but unexpectedly increased the Y397-FAK phosphorylation and intratumoral MMP9 expression (Fig. 6), suggesting inhibition of Src phosphorylation alone is insufficient to impede the activation of EMT and elevation of invasive potential associated with acquired sorafenib resistance. The upregulated Y397-FAK phosphorylation is possibly triggered by microenvironmental cues such as cytokines, growth factors, integrins and so on (Sulzmaier et al., 2014). Further studies are needed to characterize the impact of tumor microenvironment on the Src-independent FAK signal transduction pathway.

Taken together, results of this study revealed not only the contribution of FAK/Src activation to the acquired sorafenib resistance in *KRAS*-mutant A549 xenografts by promoting the EMT and invasive potential, but also the fact that Src inhibition alone was

insufficient to overcome the resistance. Given the evolving redundancy of oncogenic pathways that enable tumor cells to compensate for several targeted genes and pathways, the major challenge of overcoming acquired resistance to pathway-targeted drugs is to identify a “master switch” that regulates and coordinates multiple signaling pathways involved in the resistance. Nonetheless, this work provides an example of rational combination of two targeted therapeutic agents to combat the acquired tumor resistance to single-agent targeted therapy. Based on our findings, further investigation is warranted to identify the most effective combination therapy to maximize the therapeutic benefit of sorafenib in *KRAS*-mutant NSCLC.

Authorship Contributions

Participated in research design: Zhou

Conducted experiments: Guo, Choksi, and Zhou

Performed data analysis: Guo, and Zhou

Wrote or contributed to the writing of the manuscript: Zhou, and Guo

References

Alvarado CG, Maruyama S, Cheng J, Ida-Yonemochi H, Kobayashi T, Yamazaki M, Takagi R and Saku T (2011) Nuclear translocation of beta-catenin synchronized with loss of E-cadherin in oral epithelial dysplasia with a characteristic two-phase appearance. *Histopathology* **59**:283-291.

Blumenschein GR, Jr., Saintigny P, Liu S, Kim ES, Tsao AS, Herbst RS, Alden C, Lee JJ, Tang X, Stewart DJ, Kies MS, Fossella FV, Tran HT, Mao L, Hicks ME, Erasmus J, Jr., Gupta S, Girard L, Peyton M, Diao L, Wang J, Davis SE, Minna JD, Wistuba I, Hong WK, Heymach JV and Lippman SM (2013) Comprehensive biomarker analysis and final efficacy results of sorafenib in the BATTLE trial. *Clinical cancer research : an official journal of the American Association for Cancer Research* **19**:6967-6975.

Bromann PA, Korkaya H and Courtneidge SA (2004) The interplay between Src family kinases and receptor tyrosine kinases. *Oncogene* **23**:7957-7968.

Calautti E, Cabodi S, Stein PL, Hatzfeld M, Kedersha N and Paolo Dotto G (1998) Tyrosine phosphorylation and src family kinases control keratinocyte cell-cell adhesion. *The Journal of cell biology* **141**:1449-1465.

Chan BA and Hughes BG (2015) Targeted therapy for non-small cell lung cancer: current standards and the promise of the future. *Transl Lung Cancer Res* **4**:36-54.

Chen JS, Huang XH, Wang Q, Chen XL, Fu XH, Tan HX, Zhang LJ, Li W and Bi J (2010a) FAK is involved in invasion and metastasis of hepatocellular carcinoma. *Clinical & experimental metastasis* **27**:71-82.

Chen KF, Chen HL, Tai WT, Feng WC, Hsu CH, Chen PJ and Cheng AL (2011) Activation of phosphatidylinositol 3-kinase/Akt signaling pathway mediates acquired

resistance to sorafenib in hepatocellular carcinoma cells. *The Journal of pharmacology and experimental therapeutics* **337**:155-161.

Chen KF, Yu HC, Liu TH, Lee SS, Chen PJ and Cheng AL (2010b) Synergistic interactions between sorafenib and bortezomib in hepatocellular carcinoma involve PP2A-dependent Akt inactivation. *Journal of hepatology* **52**:88-95.

Cheng JC, Chou CH, Kuo ML and Hsieh CY (2006) Radiation-enhanced hepatocellular carcinoma cell invasion with MMP-9 expression through PI3K/Akt/NF-kappaB signal transduction pathway. *Oncogene* **25**:7009-7018.

Chou TC and Talalay P (1981) Generalized equations for the analysis of inhibitions of Michaelis-Menten and higher-order kinetic systems with two or more mutually exclusive and nonexclusive inhibitors. *Eur J Biochem* **115**:207-216.

Dingemans AM, Mellema WW, Groen HJ, van Wijk A, Burgers SA, Kunst PW, Thunnissen E, Heideman DA and Smit EF (2013) A phase II study of sorafenib in patients with platinum-pretreated, advanced (Stage IIIb or IV) non-small cell lung cancer with a KRAS mutation. *Clinical cancer research : an official journal of the American Association for Cancer Research* **19**:743-751.

Firtina Karagonlar Z, Koc D, Iscan E, Erdal E and Atabey N (2016) Elevated hepatocyte growth factor expression as an autocrine c-Met activation mechanism in acquired resistance to sorafenib in hepatocellular carcinoma cells. *Cancer science* **107**:407-416.

Ghahhari NM and Babashah S (2015) Interplay between microRNAs and WNT/beta-catenin signalling pathway regulates epithelial-mesenchymal transition in cancer. *European journal of cancer* **51**:1638-1649.

Gotz R (2008) Inter-cellular adhesion disruption and the RAS/RAF and beta-catenin signalling in lung cancer progression. *Cancer cell international* **8**:7.

Harada K, Miyake H, Kusuda Y and Fujisawa M (2014) Characterization of mechanism involved in acquired resistance to sorafenib in a mouse renal cell cancer RenCa model. *Clin Transl Oncol* **16**:801-806.

Jing Y, Han Z, Zhang S, Liu Y and Wei L (2011) Epithelial-Mesenchymal Transition in tumor microenvironment. *Cell Biosci* **1**:29.

Kageshita T, Hamby CV, Ishihara T, Matsumoto K, Saida T and Ono T (2001) Loss of beta-catenin expression associated with disease progression in malignant melanoma. *The British journal of dermatology* **145**:210-216.

Kantarjian H, Jabbour E, Grimley J and Kirkpatrick P (2006) Dasatinib. *Nature reviews Drug discovery* **5**:717-718.

Kim ES, Herbst RS, Wistuba, II, Lee JJ, Blumenschein GR, Jr., Tsao A, Stewart DJ, Hicks ME, Erasmus J, Jr., Gupta S, Alden CM, Liu S, Tang X, Khuri FR, Tran HT, Johnson BE, Heymach JV, Mao L, Fossella F, Kies MS, Papadimitrakopoulou V, Davis SE, Lippman SM and Hong WK (2011) The BATTLE trial: personalizing therapy for lung cancer. *Cancer discovery* **1**:44-53.

Lachenmayer A, Alsinet C, Savic R, Cabellos L, Toffanin S, Hoshida Y, Villanueva A, Minguez B, Newell P, Tsai HW, Barretina J, Thung S, Ward SC, Bruix J, Mazzaferro V, Schwartz M, Friedman SL and Llovet JM (2012) Wnt-pathway activation in two molecular classes of hepatocellular carcinoma and experimental modulation by sorafenib. *Clinical cancer research : an official journal of the American Association for Cancer Research* **18**:4997-5007.

Lindblad O, Cordero E, Puissant A, Macaulay L, Ramos A, Kabir NN, Sun J, Vallon-Christersson J, Haraldsson K, Hemann MT, Borg A, Levander F, Stegmaier K, Pietras K, Ronnstrand L and Kazi JU (2016) Aberrant activation of the PI3K/mTOR pathway promotes resistance to sorafenib in AML. *Oncogene* **35**:5119-5131.

Liu L, Cao Y, Chen C, Zhang X, McNabola A, Wilkie D, Wilhelm S, Lynch M and Carter C (2006) Sorafenib blocks the RAF/MEK/ERK pathway, inhibits tumor angiogenesis, and induces tumor cell apoptosis in hepatocellular carcinoma model PLC/PRF/5. *Cancer research* **66**:11851-11858.

Mahoney CL, Choudhury B, Davies H, Edkins S, Greenman C, Haaften G, Mironenko T, Santarius T, Stevens C, Stratton MR and Futreal PA (2009) LKB1/KRAS mutant lung cancers constitute a genetic subset of NSCLC with increased sensitivity to MAPK and mTOR signalling inhibition. *British journal of cancer* **100**:370-375.

McMillin DW, Negri JM and Mitsiades CS (2013) The role of tumour-stromal interactions in modifying drug response: challenges and opportunities. *Nature reviews Drug discovery* **12**:217-228.

Mitra SK, Hanson DA and Schlaepfer DD (2005) Focal adhesion kinase: in command and control of cell motility. *Nature reviews Molecular cell biology* **6**:56-68.

Morgillo F, Cascone T, D'Aiuto E, Martinelli E, Troiani T, Saintigny P, De Palma R, Heymach JV, Berrino L, Tuccillo C and Ciardiello F (2011) Antitumour efficacy of MEK inhibitors in human lung cancer cells and their derivatives with acquired resistance to different tyrosine kinase inhibitors. *British journal of cancer* **105**:382-392.

Noren NK, Niessen CM, Gumbiner BM and Burridge K (2001) Cadherin engagement regulates Rho family GTPases. *The Journal of biological chemistry* **276**:33305-33308.

Onder TT, Gupta PB, Mani SA, Yang J, Lander ES and Weinberg RA (2008) Loss of E-cadherin promotes metastasis via multiple downstream transcriptional pathways. *Cancer research* **68**:3645-3654.

Pao W and Chmielecki J (2010) Rational, biologically based treatment of EGFR-mutant non-small-cell lung cancer. *Nature reviews Cancer* **10**:760-774.

Paz-Ares L, Hirsh V, Zhang L, de Marinis F, Yang JC, Wakelee HA, Seto T, Wu YL, Novello S, Juhasz E, Aren O, Sun Y, Schmelter T, Ong TJ, Pena C, Smit EF and Mok TS (2015) Monotherapy Administration of Sorafenib in Patients With Non-Small Cell Lung Cancer (MISSION) Trial: A Phase III, Multicenter, Placebo-Controlled Trial of Sorafenib in Patients with Relapsed or Refractory Predominantly Nonsquamous Non-Small-Cell Lung Cancer after 2 or 3 Previous Treatment Regimens. *Journal of thoracic oncology : official publication of the International Association for the Study of Lung Cancer* **10**:1745-1753.

Rodriguez FJ, Lewis-Tuffin LJ and Anastasiadis PZ (2012) E-cadherin's dark side: possible role in tumor progression. *Biochimica et biophysica acta* **1826**:23-31.

Sulzmaier FJ, Jean C and Schlaepfer DD (2014) FAK in cancer: mechanistic findings and clinical applications. *Nature reviews Cancer* **14**:598-610.

Sun X, Niu X, Chen R, He W, Chen D, Kang R and Tang D (2016) Metallothionein-1G facilitates sorafenib resistance through inhibition of ferroptosis. *Hepatology* **64**:488-500.

Tai WT, Cheng AL, Shiau CW, Liu CY, Ko CH, Lin MW, Chen PJ and Chen KF (2012) Dovitinib induces apoptosis and overcomes sorafenib resistance in hepatocellular carcinoma through SHP-1-mediated inhibition of STAT3. *Molecular cancer therapeutics* **11**:452-463.

Thamilselvan V, Craig DH and Basson MD (2007) FAK association with multiple signal proteins mediates pressure-induced colon cancer cell adhesion via a Src-dependent PI3K/Akt pathway. *FASEB journal : official publication of the Federation of American Societies for Experimental Biology* **21**:1730-1741.

Thomas SM and Jordan TR (2004) Contributions of oral and extraoral facial movement to visual and audiovisual speech perception. *J Exp Psychol Hum Percept Perform* **30**:873-888.

Tovar V, Cornella H, Moeini A, Vidal S, Hoshida Y, Sia D, Peix J, Cabellos L, Alsinet C, Torrecilla S, Martinez-Quetglas I, Lozano JJ, Desbois-Mouthon C, Sole M, Domingo-Domenech J, Villanueva A and Llovet JM (2015) Tumour initiating cells and IGF/FGF signalling contribute to sorafenib resistance in hepatocellular carcinoma. *Gut*.

Ulivi P, Arienti C, Amadori D, Fabbri F, Carloni S, Tesei A, Vannini I, Silvestrini R and Zoli W (2009) Role of RAF/MEK/ERK pathway, p-STAT-3 and Mcl-1 in sorafenib activity in human pancreatic cancer cell lines. *Journal of cellular physiology* **220**:214-221.

van Malenstein H, Dekervel J, Verslype C, Van Cutsem E, Windmolders P, Nevens F and van Pelt J (2013) Long-term exposure to sorafenib of liver cancer cells induces

resistance with epithelial-to-mesenchymal transition, increased invasion and risk of rebound growth. *Cancer letters* **329**:74-83.

Van Slambrouck S, Grijelmo C, De Wever O, Bruyneel E, Emami S, Gespach C and Steelant WF (2007) Activation of the FAK-src molecular scaffolds and p130Cas-JNK signaling cascades by alpha1-integrins during colon cancer cell invasion. *International journal of oncology* **31**:1501-1508.

Wang H, Xu L, Zhu X, Wang P, Chi H and Meng Z (2014) Activation of phosphatidylinositol 3-kinase/Akt signaling mediates sorafenib-induced invasion and metastasis in hepatocellular carcinoma. *Oncology reports* **32**:1465-1472.

Westhoff MA, Serrels B, Fincham VJ, Frame MC and Carragher NO (2004) SRC-mediated phosphorylation of focal adhesion kinase couples actin and adhesion dynamics to survival signaling. *Molecular and cellular biology* **24**:8113-8133.

Wheeler DL, Dunn EF and Harari PM (2010) Understanding resistance to EGFR inhibitors-impact on future treatment strategies. *Nature reviews Clinical oncology* **7**:493-507.

Wilhelm S, Carter C, Lynch M, Lowinger T, Dumas J, Smith RA, Schwartz B, Simantov R and Kelley S (2006) Discovery and development of sorafenib: a multikinase inhibitor for treating cancer. *Nature reviews Drug discovery* **5**:835-844.

Wilhelm SM, Carter C, Tang L, Wilkie D, McNabola A, Rong H, Chen C, Zhang X, Vincent P, McHugh M, Cao Y, Shujath J, Gawlak S, Eveleigh D, Rowley B, Liu L, Adnane L, Lynch M, Auclair D, Taylor I, Gedrich R, Voznesensky A, Riedl B, Post LE, Bollag G and Trail PA (2004) BAY 43-9006 exhibits broad spectrum oral antitumor activity and targets the RAF/MEK/ERK pathway and receptor tyrosine

kinases involved in tumor progression and angiogenesis. *Cancer research* **64**:7099-7109.

Yip WK and Seow HF (2012) Activation of phosphatidylinositol 3-kinase/Akt signaling by EGF downregulates membranous E-cadherin and beta-catenin and enhances invasion in nasopharyngeal carcinoma cells. *Cancer letters* **318**:162-172.

Zhai B, Hu F, Yan H, Zhao D, Jin X, Fang T, Pan S, Sun X and Xu L (2015) Bufalin Reverses Resistance to Sorafenib by Inhibiting Akt Activation in Hepatocellular Carcinoma: The Role of Endoplasmic Reticulum Stress. *PloS one* **10**:e0138485.

Zhang PF, Li KS, Shen YH, Gao PT, Dong ZR, Cai JB, Zhang C, Huang XY, Tian MX, Hu ZQ, Gao DM, Fan J, Ke AW and Shi GM (2016) Galectin-1 induces hepatocellular carcinoma EMT and sorafenib resistance by activating FAK/PI3K/AKT signaling. *Cell death & disease* **7**:e2201.

Zhou Q, Guo P and Gallo JM (2008) Impact of angiogenesis inhibition by sunitinib on tumor distribution of temozolomide. *Clinical cancer research : an official journal of the American Association for Cancer Research* **14**:1540-1549.

Zhou Q, Lv H, Mazloom AR, Xu H, Ma'ayan A and Gallo JM (2012) Activation of alternate prosurvival pathways accounts for acquired sunitinib resistance in U87MG glioma xenografts. *The Journal of pharmacology and experimental therapeutics* **343**:509-519.

Footnotes

This work was supported by the startup fund and internal seed grant provided to Q.Z. by the University of South Florida College of Pharmacy.

JPET Fast Forward. Published on October 11, 2017 as DOI: 10.1124/jpet.117.240507
This article has not been copyedited and formatted. The final version may differ from this version.

Figure Legends

Fig.1. *In vivo* selection of A549 human lung adenocarcinoma cells resistant to sorafenib treatment and evaluation of the sorafenib-resistant A549 xenograft model. (A) Differential tumor growth rates are observed in A549 tumor-bearing mice treated with vehicle control for 6 weeks (N = 9) or 40 mg/kg of sorafenib once daily for 15 weeks (N = 10). Sorafenib-sensitive and -resistant groups are classified based on the tumor growth index value calculated as the ratio of tumor volume at the first day of treatment to that at the last day of treatment in that those with the tumor growth index value being greater than the median value of 3.6 are classified as the sorafenib-resistant animals (*N* = 5), while the rest are defined as the sorafenib-sensitive animals (*N* = 5). (B) Tumor volumes of individual study groups are shown. (C) Experimental design for the *in vivo* study that compared the antitumor activities of sorafenib in A549 and sorafenib-resistant A549 xenografts. The sorafenib-resistant A549 subclone (A549/SRFres) was derived from a sorafenib-treated animal with the fastest growing A549 xenograft. (D) Sorafenib treatment inhibits the tumor growth in both A549 and A549/SRFres xenografts. Individual animals bearing both A549 and A549/SRFres xenografts received once daily oral administration of vehicle (N = 6) and 40 mg/kg of sorafenib (N = 7) for 8 weeks. Two of the vehicle-treated animals and two of the sorafenib-treated animals were euthanized after 8 weeks of treatment, and one vehicle-treated animal was euthanized after 10 weeks of treatment, due to their tumors reaching the maximum allowed volume (i.e., 1000 mm^3). One time-matched sorafenib-treated animal was euthanized after 10 weeks of treatment. (E) Tumor growth index values are shown. Data are presented as mean ± standard error of mean (SEM). *P < 0.05 and **P < 0.01 compared with the

vehicle treated (control) animals using the independent sample *t* test. +P < 0.05 compared with the counterpart A549 xenografts using the paired sample *t* test.

Fig.2. Western blot analysis showing that sorafenib induces MMP9 expression and phosphorylation of FAK, Src and AKT and decreases the expression of E-cadherin (the epithelial marker) and β-catenin in A549 and A549/SRFres xenografts. (A) Western blot of A549 (left) and A549/SRFres (right) tumor homogenates to detect the proteins indicated. (B) Densitometric analysis shows similar trends in the effect of sorafenib on individual protein expression levels in A549 (left) and A549/SRFres (right) tumors. Relative quantification is performed, and relative immunoreactive band intensities are expressed as percent change over the average signal value in vehicle control tumors with normalization to β-actin loading controls. Error bars are standard deviations (SD). *P < 0.05 and **P < 0.01 compared with the vehicle treated (control) xenografts using the independent sample *t* test.

Fig. 3. No significant difference in the migratory and invasive phenotype between A549 parental and A549/SRFres cells. However, differential expression of phospho-Src (Y416) and phospho-FAK (Y576/577) were observed between those two cell lines. (A) Representative micrographs of scratch wound closure kinetics of cultured A549 and A549/SRFres cells. Quantification of relative wound area at 24 and 48 hr after wounding of the cell monolayers, expressed as % wound closure, demonstrated no significant difference in the migratory ability between those two cell lines *in vitro*. Error bars represent the SD of the mean from 6 independent experiments. (B) Representative micrographs from the transwell invasion assay performed by plating A549 and A549/SRFres cells on uncoated and Matrigel-coated transwell membranes. No

significant difference in the *in vitro* invasion ability between those two cells based on the percent invasion value, which was calculated as the percent of invaded cells relative to migrated cells. Error bars represent the SD of the mean from 3 independent experiments. (C) Western blot analysis demonstrated that A549/SRFres cells exhibited relatively higher baseline expression levels of phospho-Src (Y416) and phospho-FAK (Y576/577) than A549 cells. Sorafenib had little effect on Src and FAK phosphorylation, whereas dasatinib drastically decreased the levels of phospho-Src (Y416) and phospho-FAK (Y576/577) in both A549 and A549/SRFres cells. Relative densitometric quantification is performed. For phosphorylated proteins, the ratio of phosphorylated:total species was determined. For other proteins, relative protein levels were normalized to the densitometry values of β-actin.

Fig.4. Sorafenib and dasatinib, alone and in combination, inhibit A549 and A549/SRFres cell growth *in vitro* and *in vivo*. (A) Composite dose-effect curves for *in vitro* antiproliferative activity of sorafenib and dasatinib alone (0 – 100 μM) and in combination (at fixed molar ratios of sorafenib/dasatinib = 1:3, 1:1 and 3:1) in A549 (top left) and A549/SRFres (middle left) cells. Error bars are inter-assay SD. (B) The corresponding combination index for the sorafenib-dasatinib interaction in A549 and A549/SRFres cells as a function of fraction affected. (C) Antitumor activity of sorafenib and dasatinib, as single agents or in combination, in A549 (top right) and A549/SRFres (bottom right) xenografts. Mice bearing subcutaneous A549 and A549/SRFres tumors were treated with oral administration of 40 mg/kg of sorafenib, 40 mg/kg of dasatinib or the combination of the two agents at half of the doses for 4 weeks. Values indicate mean ± SEM. *P < 0.05 and **P < 0.01 compared with the vehicle treated (control)

JPET Fast Forward. Published on October 11, 2017 as DOI: 10.1124/jpet.117.240507
This article has not been copyedited and formatted. The final version may differ from this version.

animals. #P < 0.05 and ##P < 0.01 compared with the dasatinib-treated animals using Kruskal-Wallis one-way analysis of variance on ranks followed by the post-hoc Kruskal-Wallis multiple comparison z-value test. +P < 0.05 and ++ P < 0.01 compared with the counterpart A549 xenografts using the paired sample *t* test.

Fig.5. Immunohistochemical analyses of A549 and A549/SRFres xenografts. Tumors were harvested from individual mice bearing both A549 and A549/SRFres xenografts after 28 days of treatment with either vehicle control (N = 6), or sorafenib alone (40mg/kg/d, N = 7), or dasatinib alone (40mg/kg/d, N = 7), or sorafenib in combination with dasatinib (20 mg/kg/d for each, N = 8). (A) Representative images for Immunofluorescence double staining for CD31 (green), plus Ki67 (red), E-cadherin (red), collagen IV (red), or α-SMA (red) in tumor sections from individual study groups. The nuclei were stained with DAPI. Original magnifications, × 200. (B) Quantification of Ki67 immunofluorescence staining shown by the percentage of Ki67-positive cells compared to total number of cells per field. (C) Quantification of E-cadherin immunofluorescence staining shown by the percentage of E-cadherin positive area compared to the tumor area per field. (D) Quantification of immunofluorescence staining for microvessel baseline membrane shown by the percentage of collagen IV-stained area per field. (E) Quantification of collagen IV immunofluorescence staining for mural cells shown by the percentage of α-SMA-stained area per field. (F) Quantification of immunofluorescence staining for microvessel density (MVD) shown by the percentage of CD31-stained area per field. Error bars are SD. *P < 0.05 and **P < 0.01 using Kruskal-Wallis one-way analysis of variance on ranks followed by the post-hoc Kruskal-Wallis multiple comparison z-value test. +P < 0.05 using paired-sample *t* test.

JPET Fast Forward. Published on October 11, 2017 as DOI: 10.1124/jpet.117.240507
This article has not been copyedited and formatted. The final version may differ from this version.

Fig.6. Western blot analyses were performed to compare protein expression levels among individual study groups and between matched pairs of A549 and A549/SRFres tumors. (A), (B), (C) and (D) Quantification of Western blots by image densitometry demonstrated that sorafenib-dasatinib combination therapy blocks AKT and Src phosphorylation, which is induced by sorafenib monotherapy in A549 and A549/SRFres tumors, but fails to decrease the expression of phospho-FAK (Y397), MMP9 and vimentin. Relative immunoreactive band intensities are expressed as percent change over the average signal value in vehicle control tumors, with normalization to β-actin loading controls. For phosphorylated proteins, results are expressed as the ratio of phosphorylated-to-total species relative to the control tumor. (E) and (F) Comparison between the matched pairs of A549 and A549/SRFres tumors reveals significant decrease in expression of phospho-ERK and E-cadherin in sorafenib-treated A549/SRFres tumors, and significant decrease in MMP9 and phospho-GSK3β in dasatinib- and combination-treated A549/SRFres tumors, respectively. Values indicate mean ratio of protein expression level in A549/SRFres tumor to that in A549 tumor ± standard deviation. Error bars are SD. *P < 0.05 and **P < 0.01 using Kruskal-Wallis one-way analysis of variance on ranks followed by the post-hoc Kruskal-Wallis multiple comparison z-value test. +P < 0.05 and ++ P < 0.01 compared with the counterpart A549 xenografts using the paired sample *t* test.

JPET Fast Forward. Published on October 11, 2017 as DOI: 10.1124/jpet.117.240507
This article has not been copyedited and formatted. The final version may differ from this version.

Table 1. Sorafenib and dasatinib concentrations in plasma and tumors at 4 hour after the last dose

	Dasatinib (40 mg/kg/d) *N* = 8	**Sorafenib (40 mg/kg/d) *N* = 7**	**Dasatinib (20 mg/kg/d) + Sorafenib (20 mg/kg/d) *N* = 8**
$C_{4h,plasma}$ (μM)			
Dasatinib	1.16 ± 0.32		0.67 ± 0.48
Sorafenib		13.85 ± 4.04	5.38 ± 2.53
$C_{4h,A549\ xenograft}$ (μM)			
Dasatinib	2.70 ± 1.35		1.74 ± 0.59
Sorafenib		7.74 ± 2.83	4.15 ± 1.36
$C_{4h,A549\ xenograft}$: $C_{4h,plasma}$ ratio			
Dasatinib	2.32 ± 4.27		3.18 ± 1.54
Sorafenib		0.57 ± 0.20	0.84 ± 0.33
$C_{4h,A549/SRFres\ xenograft}$ (μM)			
Dasatinib	3.34 ± 1.74		1.82 ± 0.68
Sorafenib		9.39 ± 4.39	3.24 ± 1.89
$C_{4h,A549/SRFres\ xenograft}$: $C_{4h,plasma}$ ratio			
Dasatinib	2.87 ± 5.51		3.24 ± 1.59
Sorafenib		0.69 ± 0.33	0.61 ± 0.32

Note: Data are presented as mean ± SD.

JPET Fast Forward. Published on October 11, 2017 as DOI: 10.1124/jpet.117.240507
This article has not been copyedited and formatted. The final version may differ from this version.

Fig. 1

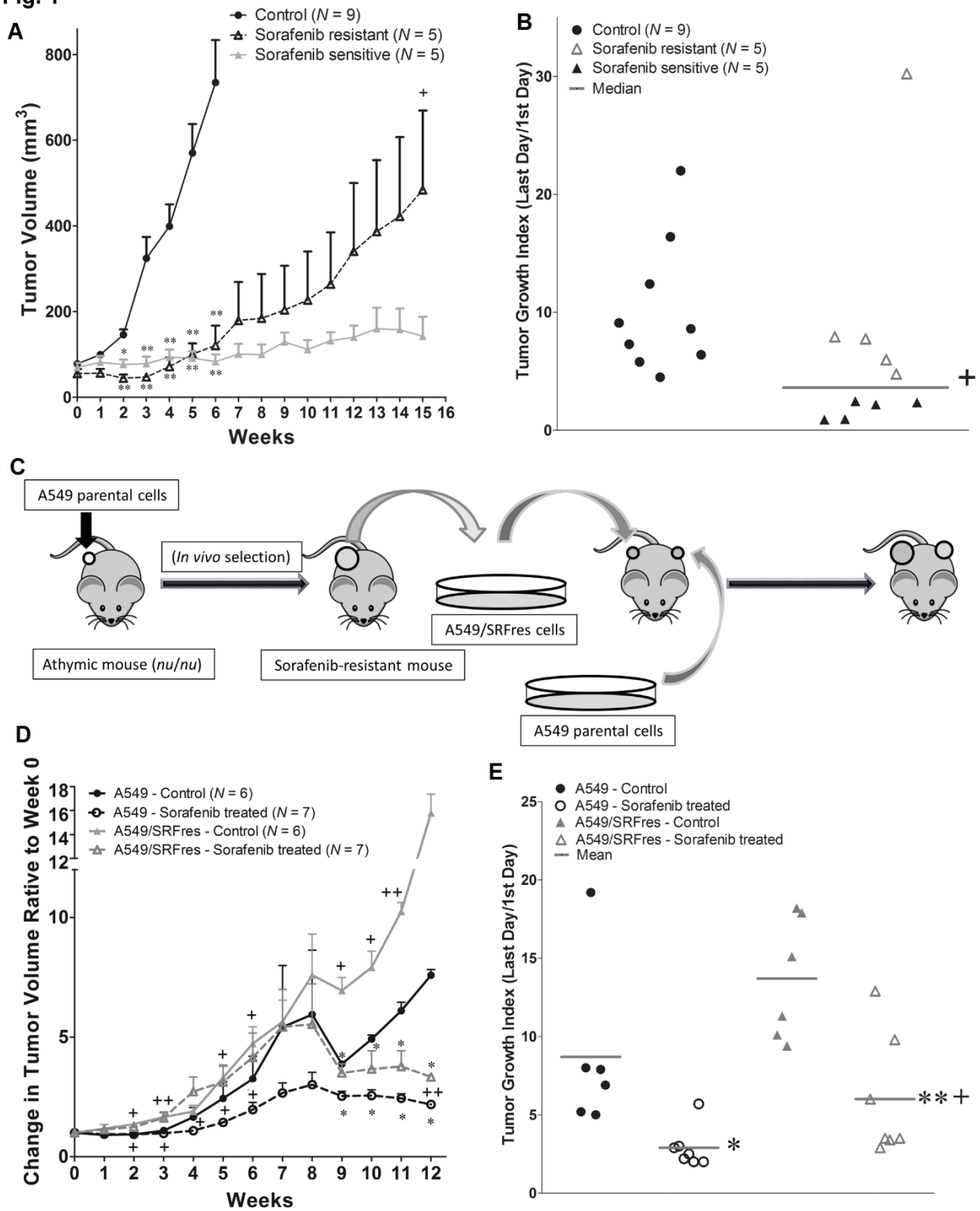

JPET Fast Forward. Published on October 11, 2017 as DOI: 10.1124/jpet.117.240507
This article has not been copyedited and formatted. The final version may differ from this version.

Fig. 2

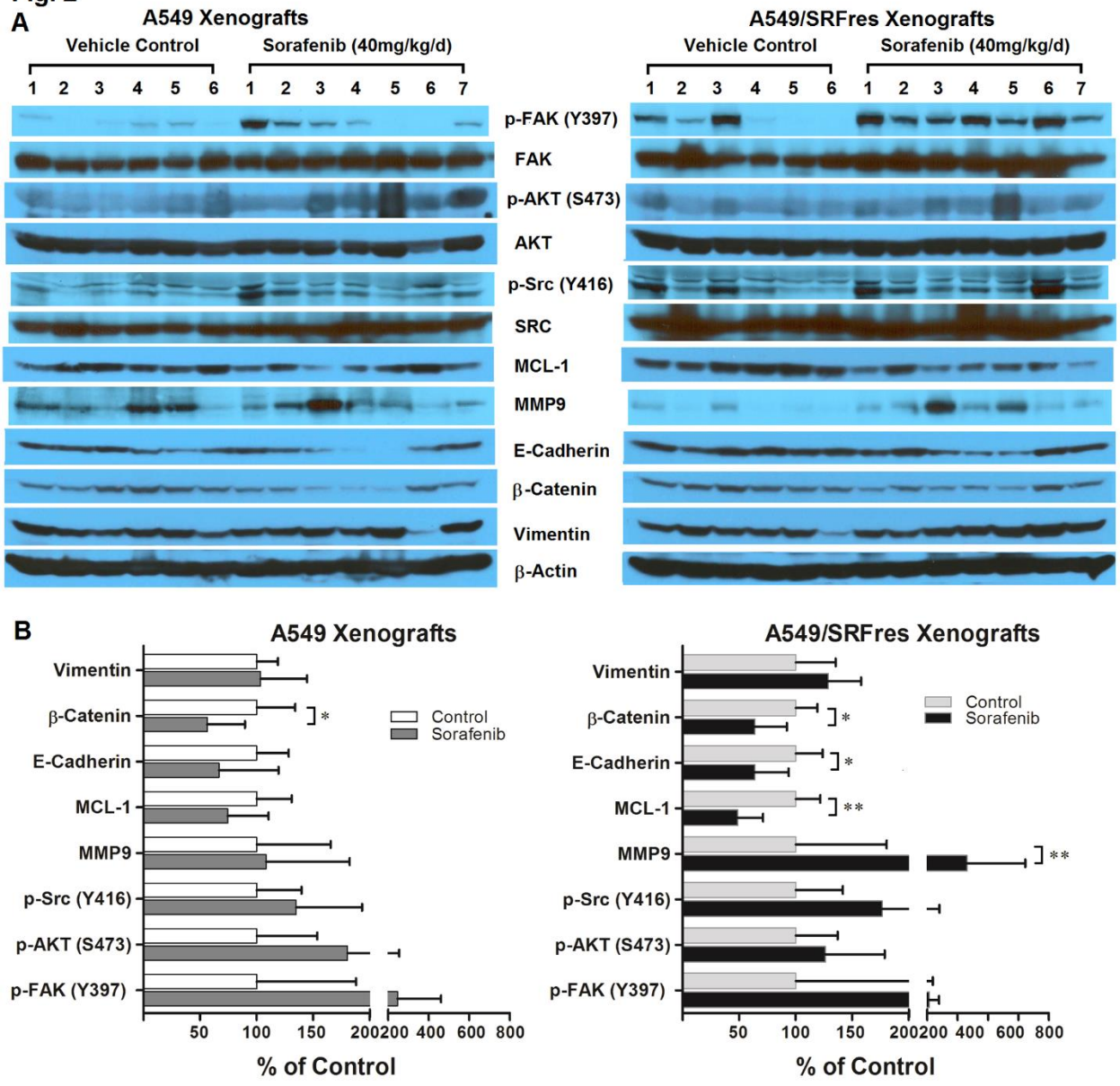

JPET Fast Forward. Published on October 11, 2017 as DOI: 10.1124/jpet.117.240507
This article has not been copyedited and formatted. The final version may differ from this version.

Fig. 3

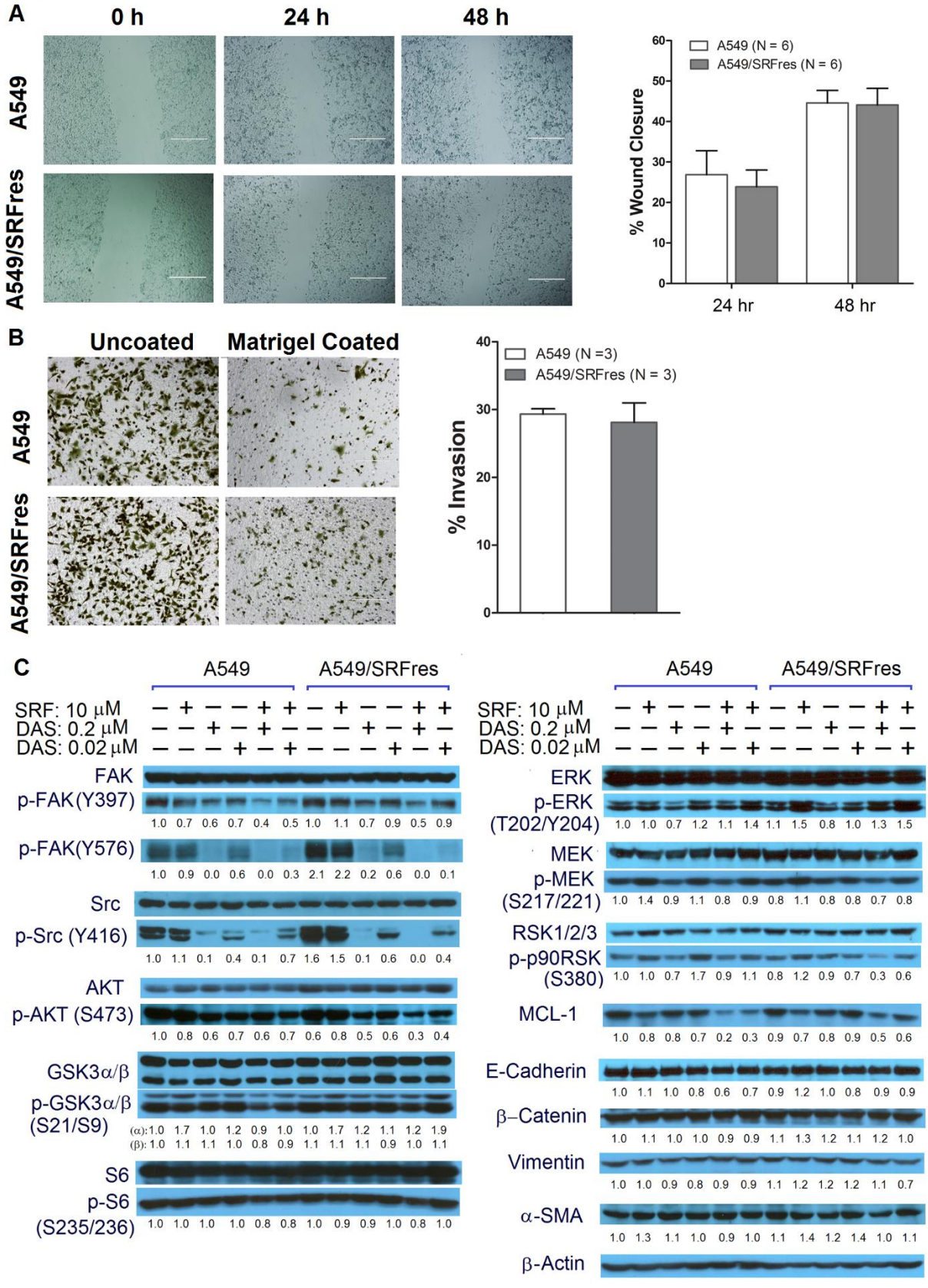

JPET Fast Forward. Published on October 11, 2017 as DOI: 10.1124/jpet.117.240507
This article has not been copyedited and formatted. The final version may differ from this version.

Fig. 4

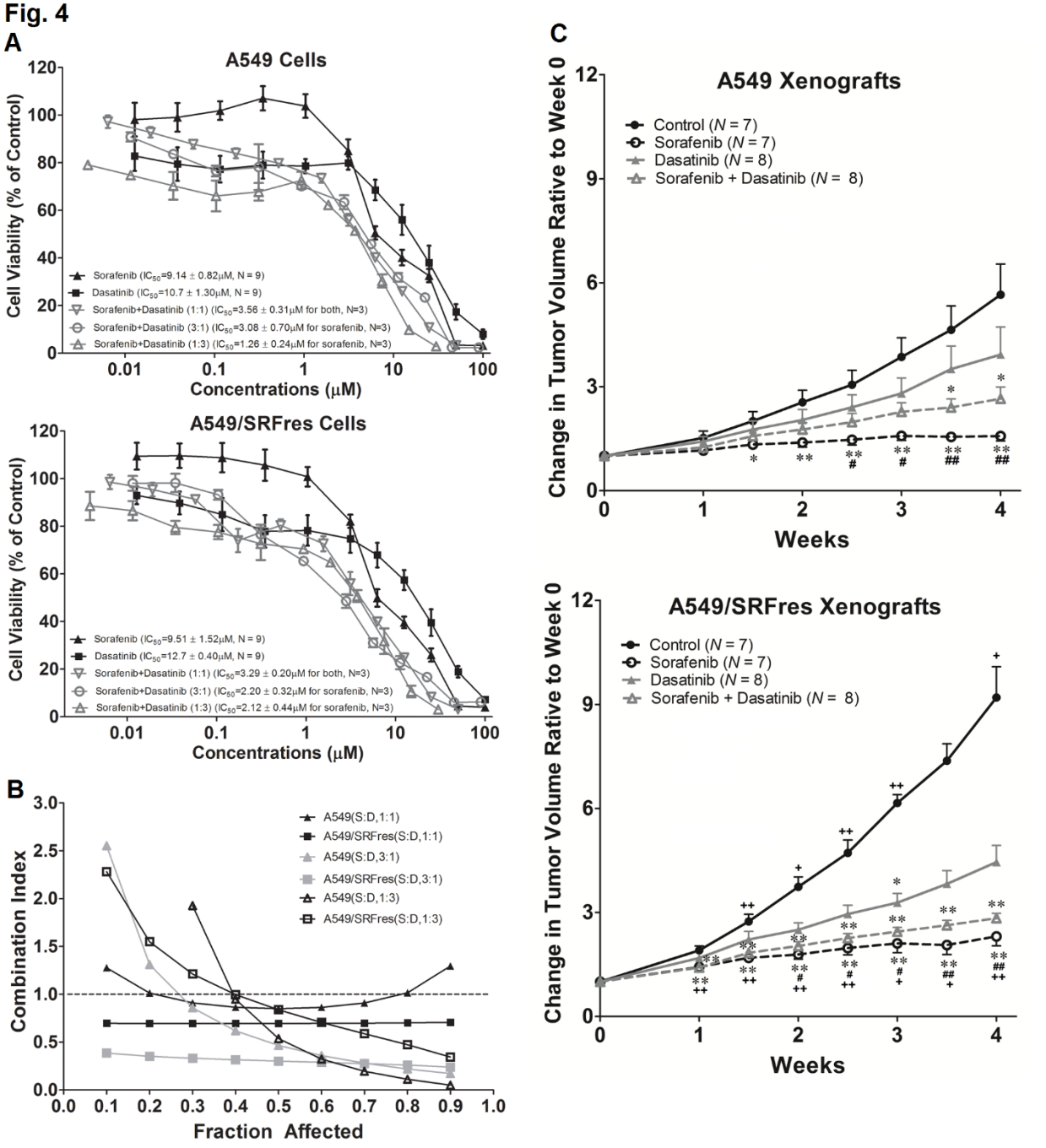

JPET Fast Forward. Published on October 11, 2017 as DOI: 10.1124/jpet.117.240507
This article has not been copyedited and formatted. The final version may differ from this version.

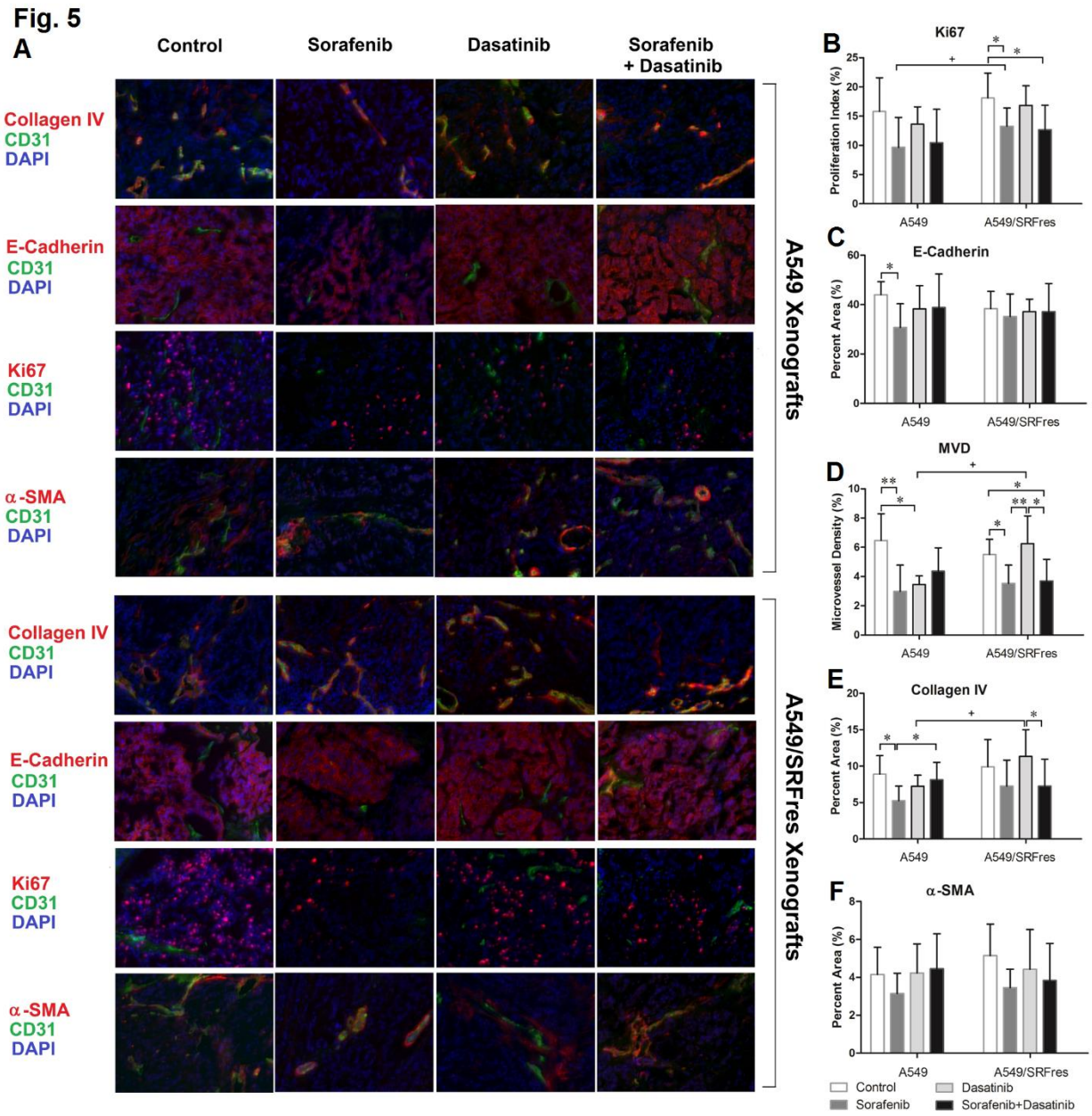

JPET Fast Forward. Published on October 11, 2017 as DOI: 10.1124/jpet.117.240507
This article has not been copyedited and formatted. The final version may differ from this version.

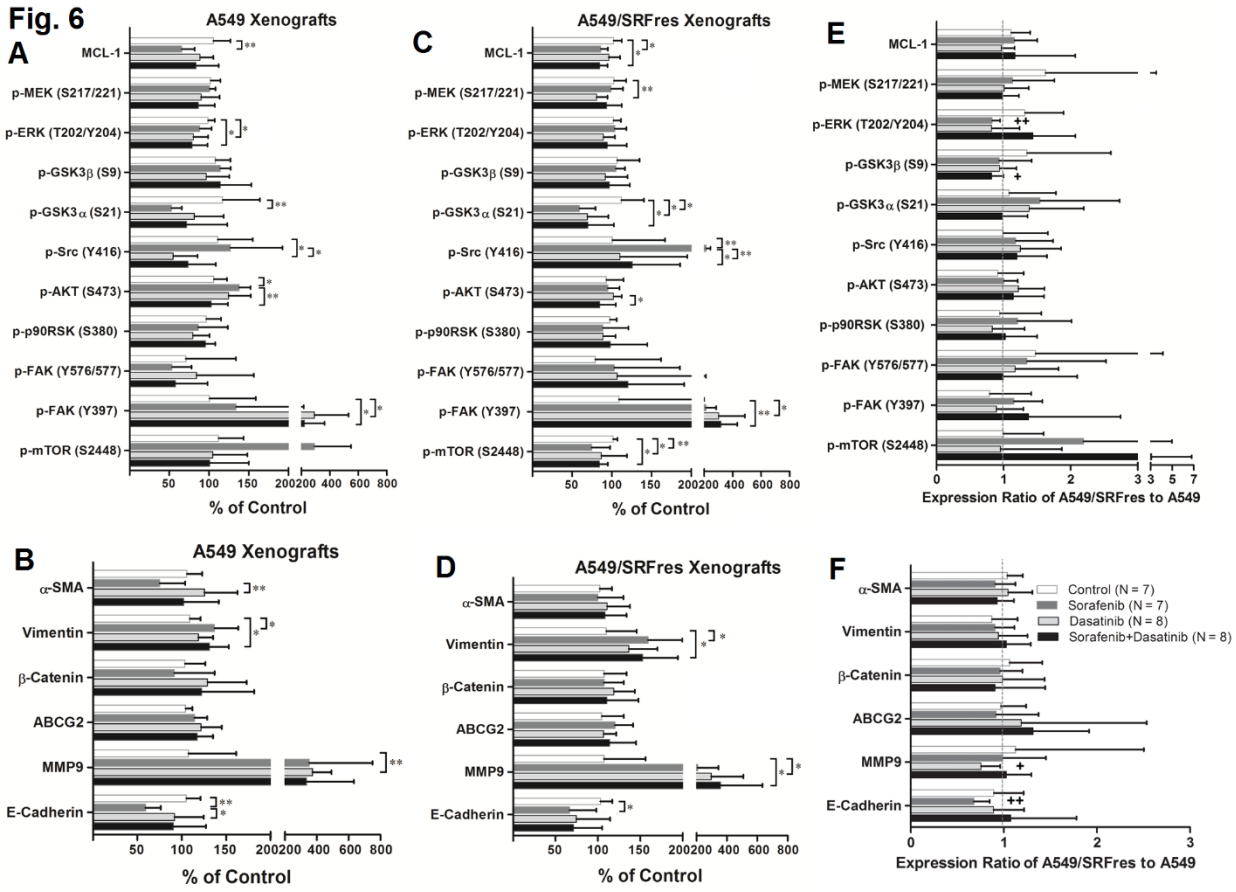

Supplemental Data

Activation of FAK and Src mediates acquired sorafenib resistance in A549 human lung adenocarcinoma xenografts

Qingyu Zhou, Xiaofang Guo, Riya Choksi

Department of Pharmaceutical Sciences, College of Pharmacy, University of South Florida, Tampa, FL 33612 (Q.Z., X.G., R.C.)

Journal of Pharmacology and Experimental Therapeutics

Supplemental Methods

In Vitro Comparison of Doubling Time between A549 and A549/SRFres Cells

Parental A549 and A549/SRFres cells in exponential growth were harvested and seeded in 96-well plates with 5 × 10^3 cells in 100 μL of complete culture medium per well and incubated at 37°C in 5% CO_2-air. Twenty-four hours after cell inoculation, cell growth curves were established by daily sampling from randomly selected wells (N = 3~4 wells per time point per cell line per experiment) for 3 consecutive days. A single cell suspension was obtained by harvesting cells with 0.05% trypsin and 1 mM EDTA (Mediatech Inc. Herndon, VA). The number of viable cells excluding trypan blue was counted on a hemocytometer under an inverted microscope (EVOS® XL Cell Imaging System, Life Technologies). Cell doubling times were calculated using the formula: $Doubleing\ Time = {}^{ln2}/_{GR}$, where GR is the growth rate constant, which was estimated using the following exponential model (Tannock, 1992): $[Cell\ number\ at\ Time\ t] = [Cell\ number\ at\ Time\ 0] \times e^{(GR \times t)}$.

Wound-Healing Assay

Wound-healing assay was used to determine cell migration as described previously with little modification (Xu and Deng, 2006). Briefly, parental A549 and A549/SRFres cells were grown in complete medium in 96-well plates to confluence. The cell monolayer was scratched with sterilized p-10 pipette tips, washed three times with PBS, and incubated in serum-free DMEM/F12 medium at 37°C in 5% CO_2-air. The recovery of the wounded monolayers due to cell migration into denuded areas was evaluated at 0, 24, and 48 hours using an EVOS® XL cell imaging system (10× objective). The area of

wound was quantified by the ImageJ software (http://rsb.info.nih.gov). Wound healing at each indicated time point was expressed as percent wound closure, which was calculated as: $\%\ Wound\ Closure = \left(1 - \frac{Area_{at\ time\ t}}{Area_{0h}}\right) \times 100\%$

Cell Invasion Assay

To assess the invasive ability of parental A549 and A549/SRFres cells, a Matrigel invasion assay was carried out in 24-well modified Boyden chambers with 8-μm pore polycarbonate filters (Corning Costar, Cambridge, MA) that were pre-coated with (invasion) or without (migration) 300 μg/ml of Growth Factor Reduced Corning® Matrigel® Matrix (Cat. No. 354230. Corning). A549 and A549/SRFres cells (2.5 × 10^4 cells per filter insert) in serum-free DMEM/F12 medium were loaded into the upper chamber with DMEM/F12 culture medium with 10% FBS in the lower chamber as a chemoattractant. After 14 hour incubation, noninvasive or non-migratory cells on the upper surface of the filter membrane were wiped out with a cotton swab, while the invaded or migratory cells on the lower surface of the filter membrane were fixed with 4% paraformaldehyde (PFA) for 10 min, stained with 0.1% crystal violet (Thermo Fisher Scientific) for 30 min and counted at 20× magnification in 5 randomly selected fields per insert. Invasiveness was determined based on percent invasion, which was calculated as: $\%\ Invasion = \frac{Mean\ number\ of\ cells\ invading\ through\ the\ Matrigel-coated\ membrane}{Mean\ number\ of\ cells\ migrating\ through\ the\ uncoated\ membrane}$

In Vivo Evaluation of Antitumor Activity of Sorafenib and Dasatinib as Single Agent at the Dose Level of 20 mg/kg

Three weeks after individual athymic nude mice were injected subcutaneously with A549 and A549/SRFres cells (5×10^6) on the left and right franks, respectively, those tumor-bearing animals were randomly divided into three groups: (1) vehicle control (N = 4), (2) 20 mg/kg/d sorafenib (N = 7) and (3) 20 mg/kg/d dasatinib (N = 8) groups. Individual animals were given once daily oral administration of either vehicle or therapeutic agents for 28 consecutive days. Body weight and tumor volume were measured twice a week throughout the treatment period. On the last day of the treatment period, animals were euthanized and the tumor mass was immediately excised, snap frozen on dry ice, and stored at –80^{o}C before subjected to Western blot analysis.

References:

Tannock IF (1992) *Cell proliferation, in The Basic Science of Oncology 2nd ed (Tannock IF, and Hill RP eds) pp 154-177*. McGraw-Hill, Inc., New York.

Xu L and Deng X (2006) Suppression of cancer cell migration and invasion by protein phosphatase 2A through dephosphorylation of mu- and m-calpains. *The Journal of biological chemistry* **281**:35567-35575.

Supplemental Tables

Supplemental Table S1. Mean combination index (CI) values of sorafenib and dasatinib used in combination.

Molar ratio of sorafenib:dasatinib	Mean CI values					
	A549 Cells			A549/SRFres Cells		
	IC_{50}	IC_{75}	IC_{90}	IC_{50}	IC_{75}	IC_{90}
1:1	0.85	0.95	1.30	0.70	0.70	0.71
3:1	0.47	0.25	0.17	0.30	0.27	0.24
1:3	0.54	0.15	0.05	0.84	0.53	0.34

Supplemental Figures

Visual Abstract

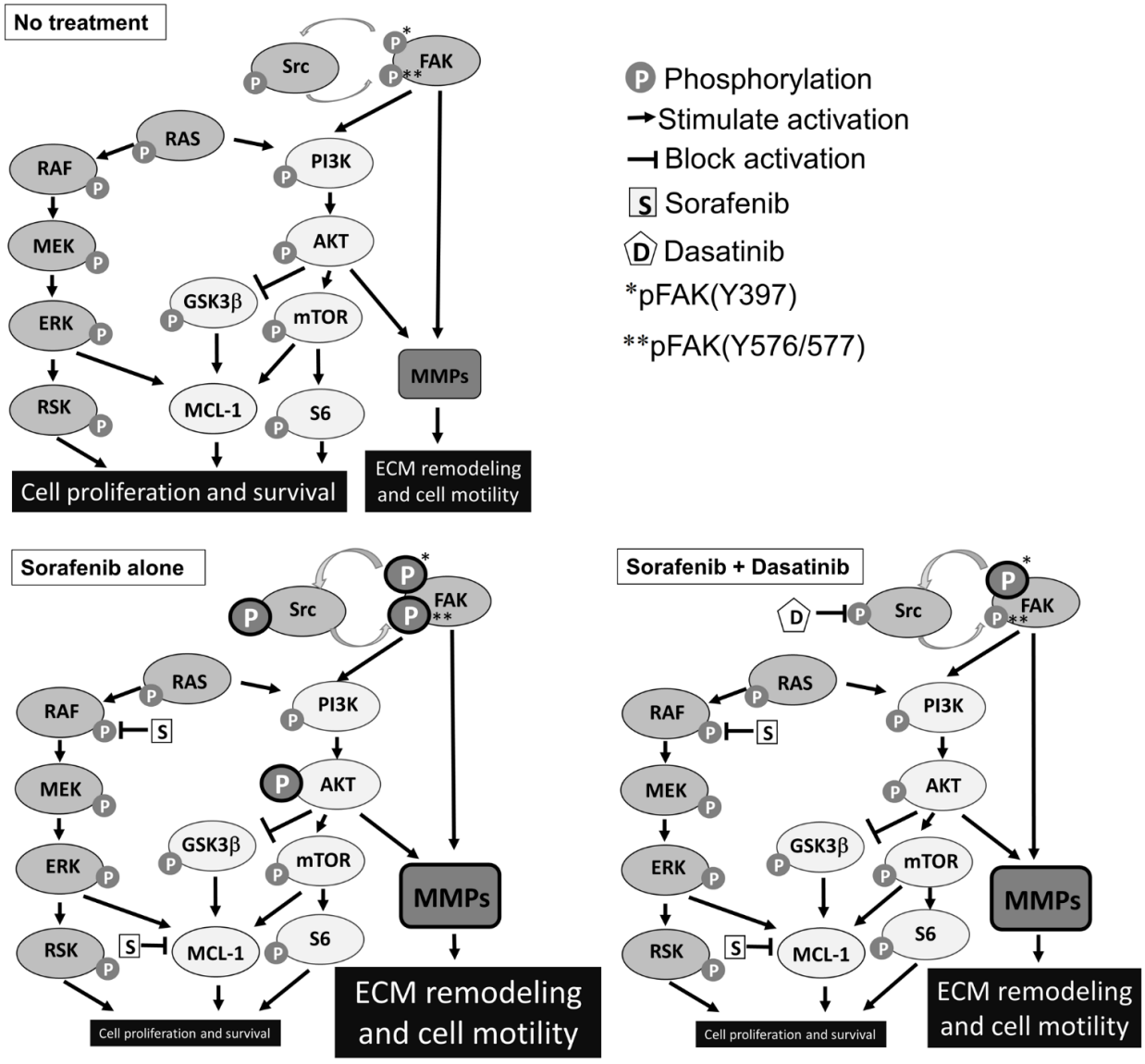

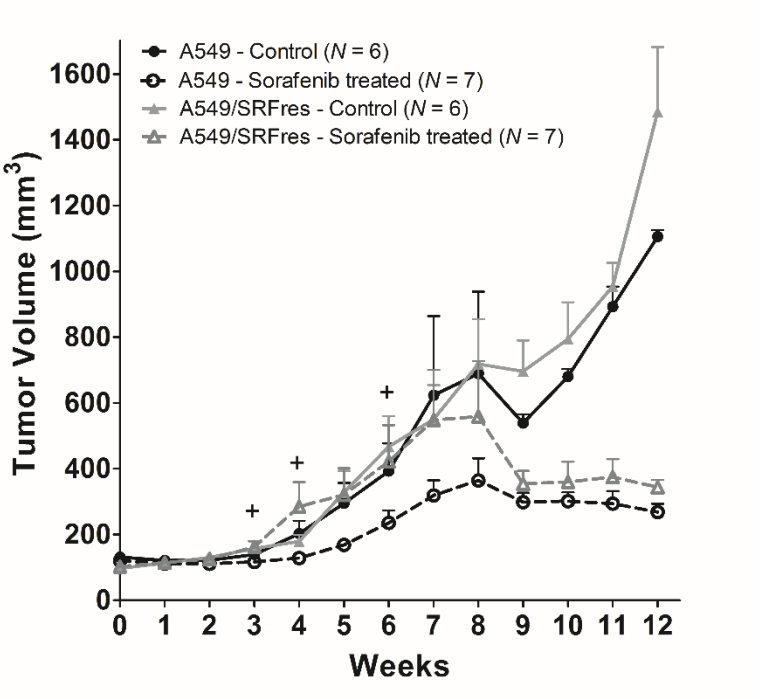

Supplemental Figure S1. Comparison of mean tumor volume values among vehicle- and sorafenib-treated A549 and A549/SRFres tumors. No significant difference was found in the mean tumor volume values among individual study groups at the start of the treatment. Data are presented as mean ± standard error of mean (SEM). *P < 0.05 and **P < 0.01 compared with the vehicle control animals using the independent sample *t* test. +P < 0.05 compared with the counterpart A549 xenografts using the paired sample *t* test.

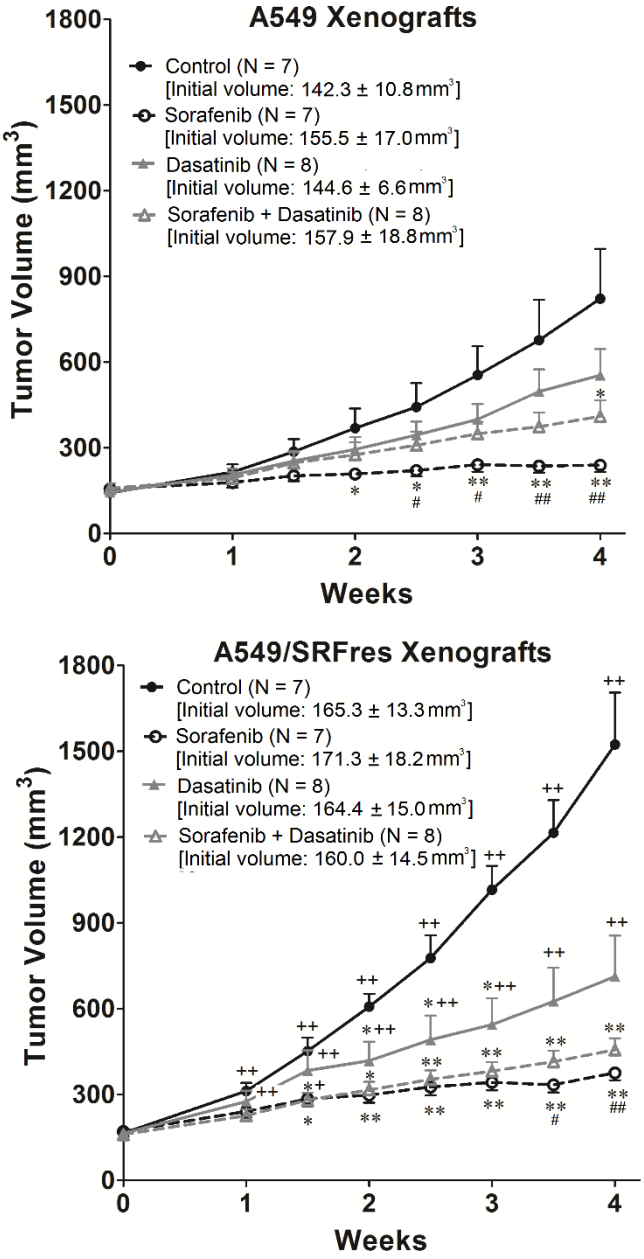

Supplemental Figure S2. Comparison of mean tumor volume values of A549 and A549/SRFres xenografts among the following study groups: vehicle control, sorafenib 40 mg/kg/d sorafenib, 40mg/kg/d dasatinib, and half-dose sorafenib-dasatinib combination groups. No significant difference was found in the mean tumor volume values among individual study groups at the start of the treatment. Values indicate mean ± SEM. *P < 0.05 and **P < 0.01 compared with the vehicle treated (control) animals, and #P < 0.05 and ##P < 0.01 compared with the dasatinib-treated animals using Kruskal-Wallis one-way analysis of variance on ranks followed by the post-hoc Kruskal-Wallis multiple comparison z-value test. +P < 0.05 and ++P < 0.01 compared with the counterpart A549 xenografts using the paired sample *t* test.

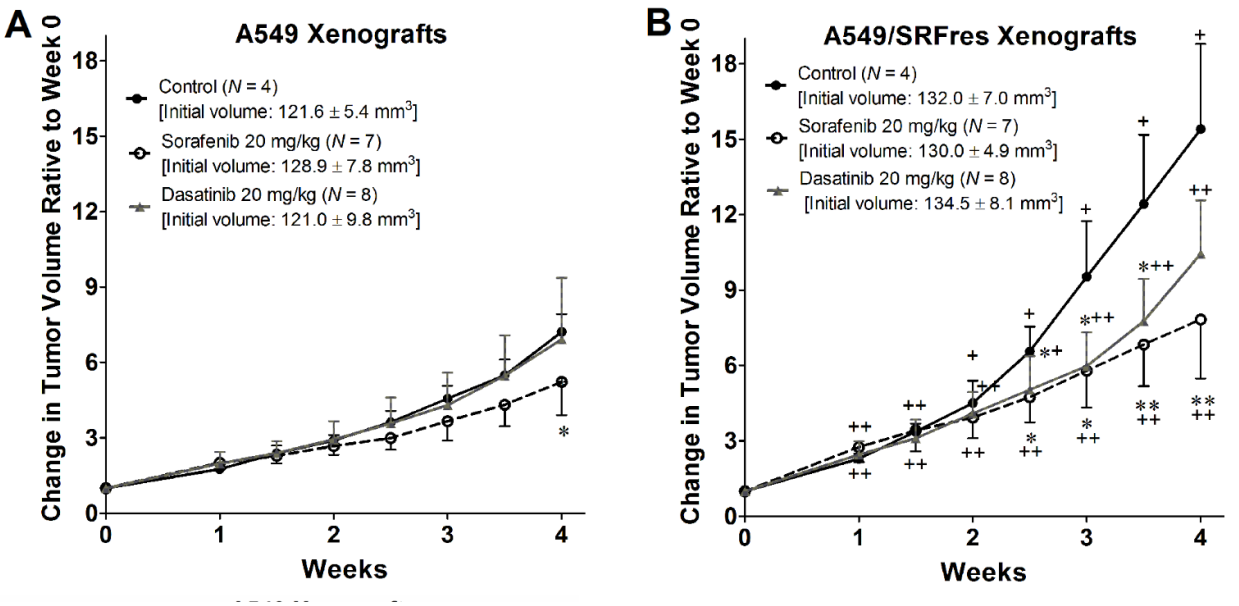

Supplemental Figure S3. Evaluation of antitumor activity of sorafenib and dasatinib, as single agents at the dose level of 20 mg/kg/d, in A549 (**A**) and A549/SRFres (**B**) xenografts. Mice bearing subcutaneous A549 and A549/SRFres tumors were treated with oral administration of 20 mg/kg of sorafenib or 20 mg/kg of dasatinib for 4 weeks. Values indicate mean ± SEM. *P < 0.05 and **P < 0.01 compared with the vehicle treated (control) animals using Kruskal-Wallis one-way analysis of variance on ranks followed by the post-hoc Kruskal-Wallis multiple comparison z-value test. +P < 0.05 and ++ P < 0.01 compared with the counterpart A549 xenografts using the paired sample *t* test.

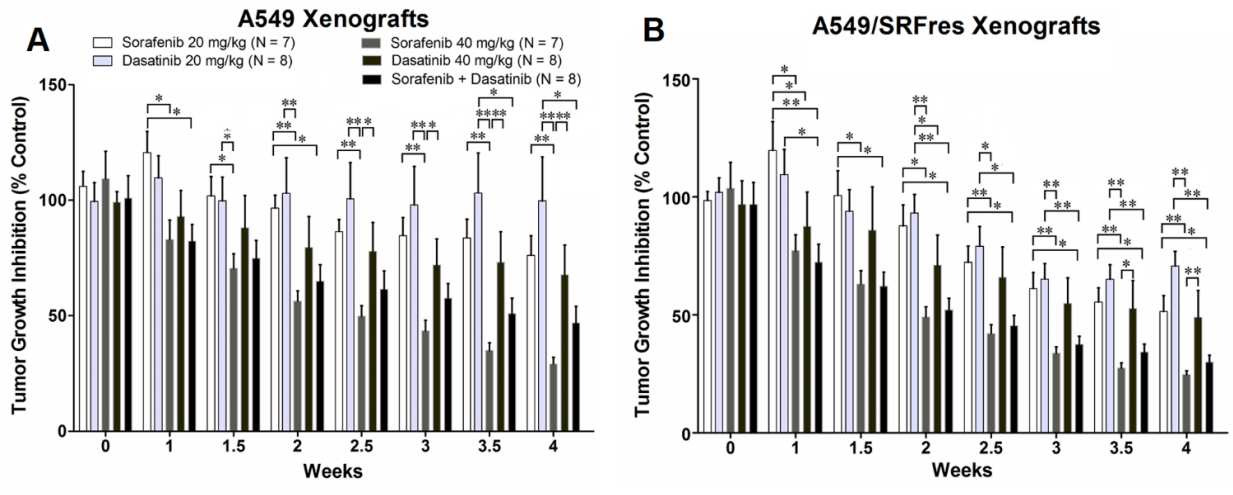

Supplemental Figure S4. Comparison of growth inhibition of A549 (**A**) and A549/SRFres (**B**) xenografts, expressed as percent of control tumor volume, among all treatment groups. The *in-vivo* anti-tumor effect of half-dose sorafenib-dasatinib combination therapy was inferior to that of the 40 mg/kg/d sorafenib treatment but superior to that of 20 mg/kg/d sorafenib, 20 mg/kg/d and 40 mg/kg/d dasatinib treatment regardless of tumor types. *P < 0.05 and **P < 0.01 using Kruskal-Wallis one-way analysis of variance on ranks followed by the post-hoc Kruskal-Wallis multiple comparison z-value test.

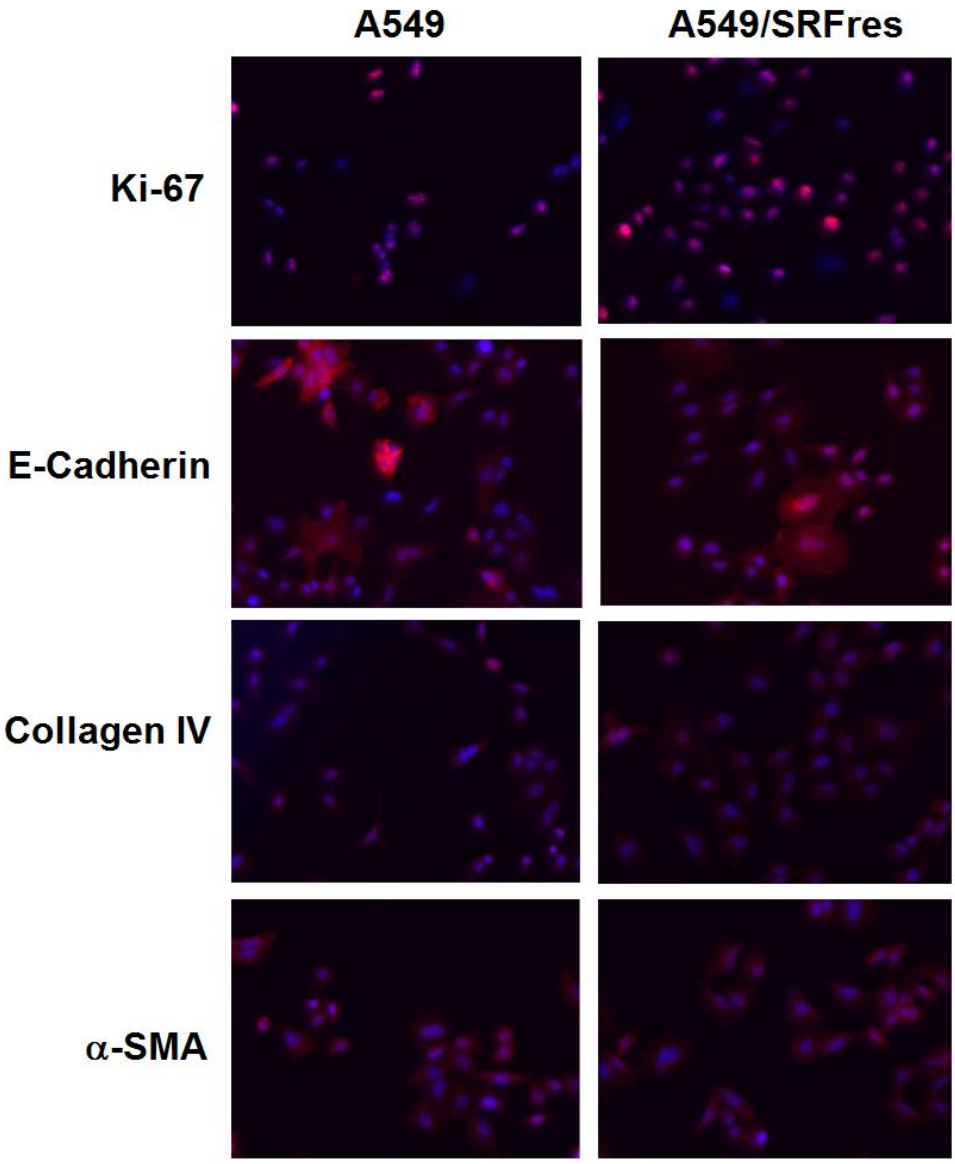

112

113 **Supplemental Figure S5.** Immunofluorescence microscopy of Ki-67, E-cadherin,
114 collagen IV and α-SMA expression in cultured A549 parental and A549/SRFres cells.

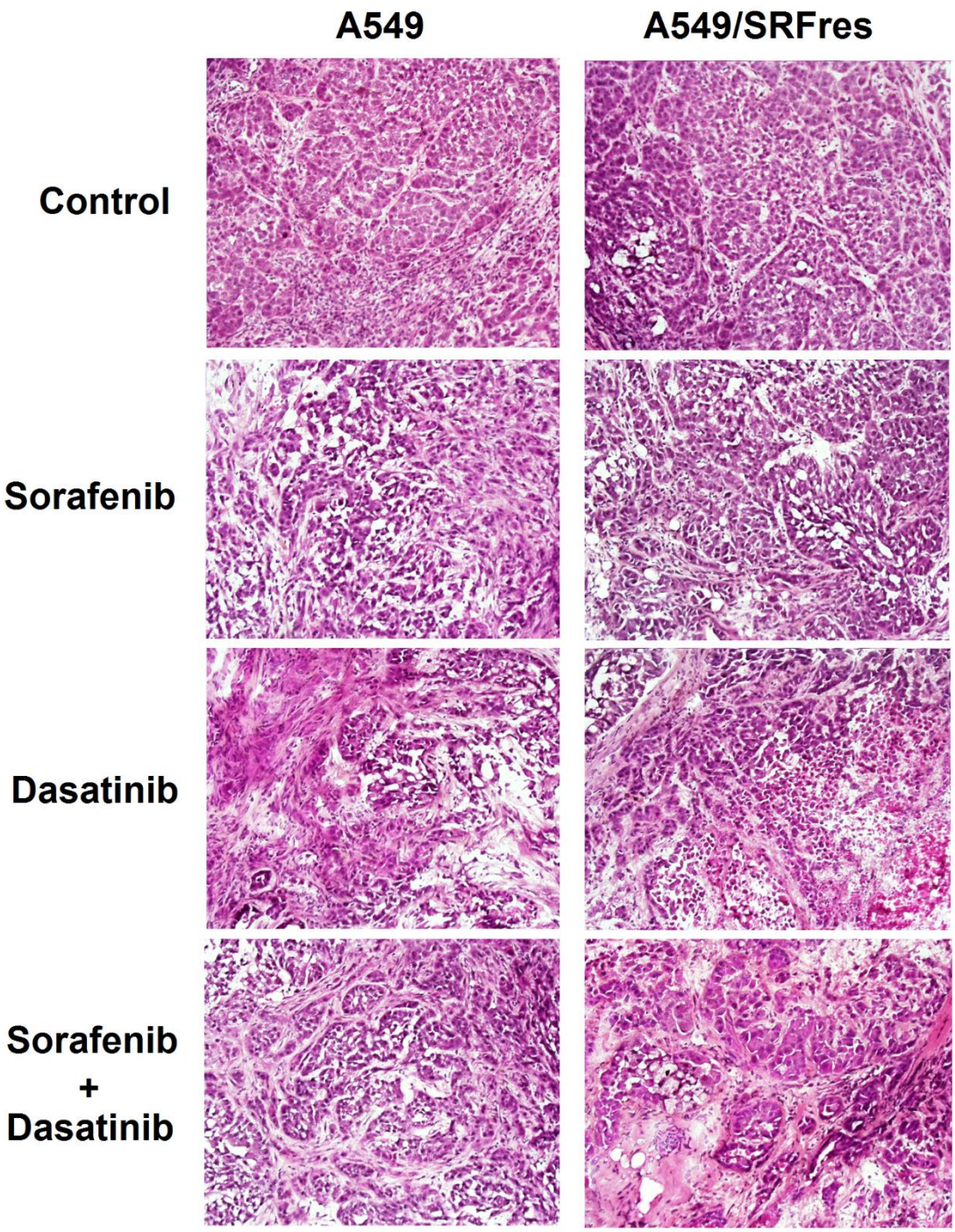

115

116 **Supplemental Figure S6.** Representative H&E-stained sections from vehicle- and
117 sorafenib-, dasatinib- and sorafenib-dasatinib-combination-treated A549 and
118 A549/SRFres tumors. All tumors showed signs of necrosis.

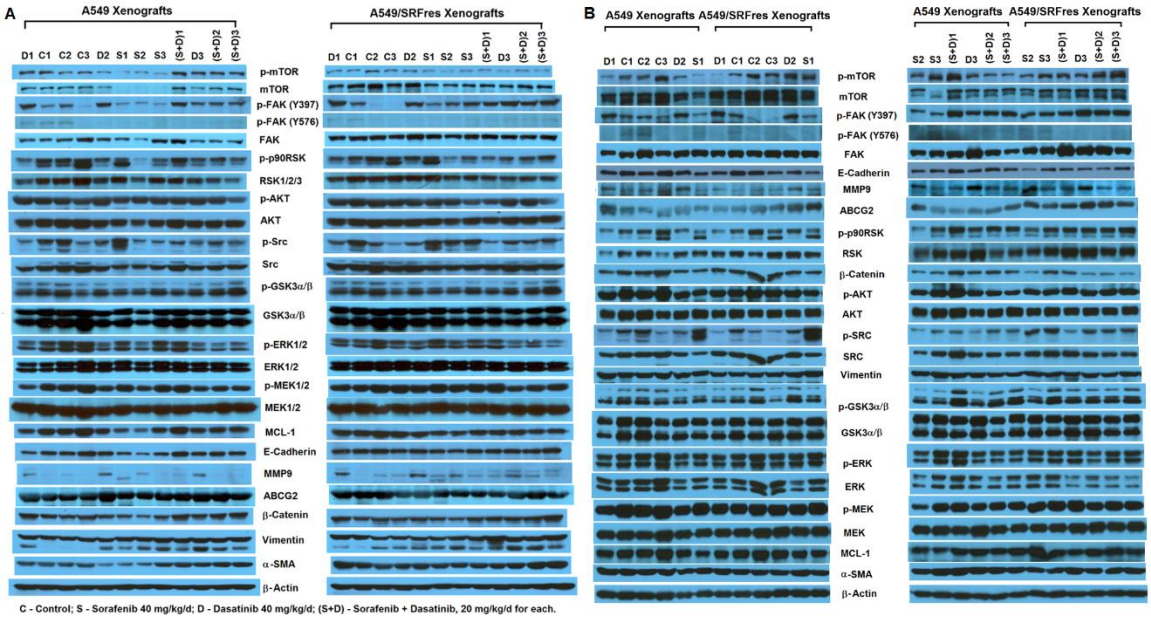

Supplemental Figure S7. Western blot analyses were performed to determine the expression levels of selected proteins involved in the signaling pathways targeted by sorafenib and dasatinib, or indicating the EMT activity and tumor cell invasive potential. Representative Western blot images reflect the differential expression of indicated proteins in A549 and A549/SRFres tumors treated with vehicle control, or 40 mg/kg/d sorafenib, or 40 mg/kg/d dasatinib, or half-dose sorafenib-dasatinib combination. Comparison of protein expression levels was made (A) among individual treatment groups of the same tumor type (either A549 or A549/SRFres tumors), and (B) between matched pairs of A549 and A549/SRFres tumors.

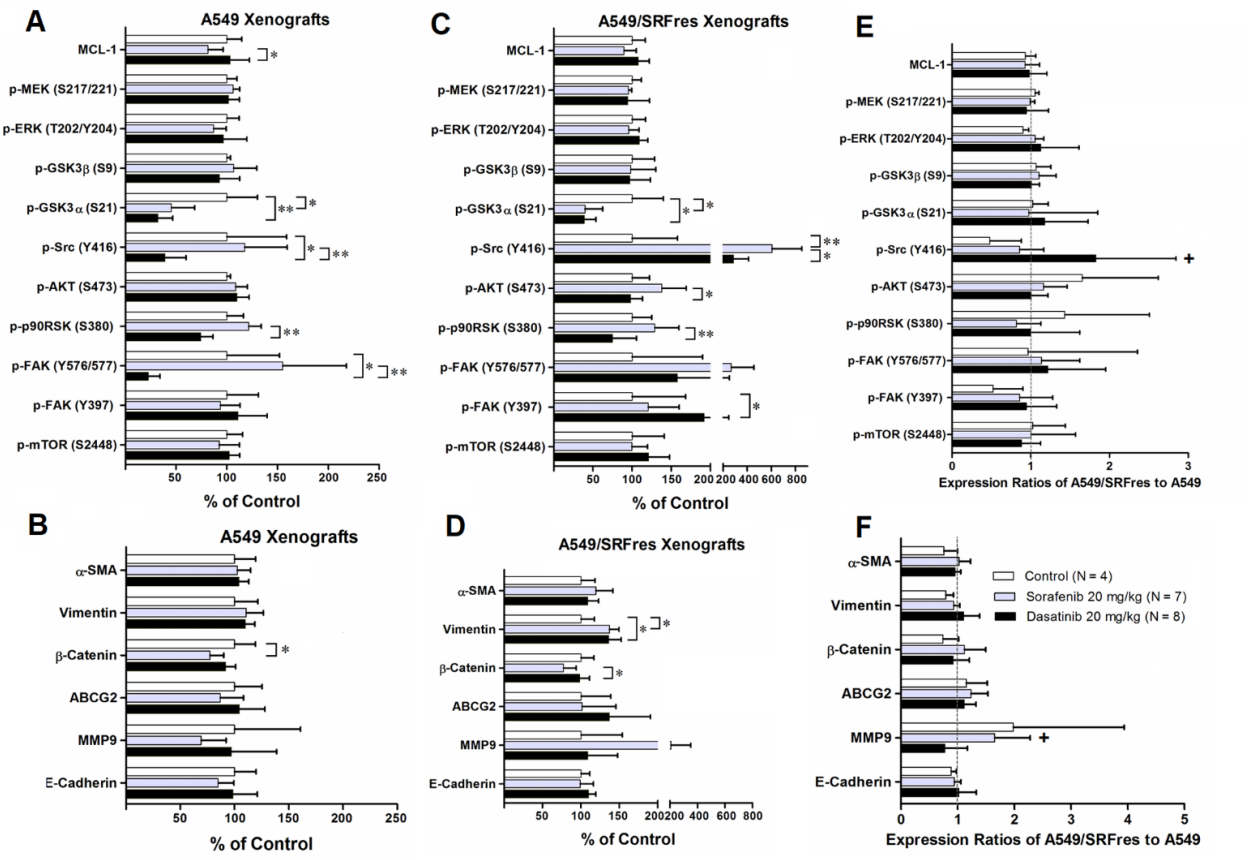

Supplemental Figure S8. (**A**), (**B**), (**C**) and (**D**) Quantification of Western blot images using the densitometric analysis shows that 20 mg/kg/d sorafenib treatment induces MMP9 and vimentin expression and phosphorylation of Src, while 20 mg/kg/d dasatinib treatment decreases the phosphorylation of SRC but increase the Y397 phosphorylation of FAK and induces vimentin expression in A549/SRFres xenografts. Both 20 mg/kg/d sorafenib and dasatinib treatments significantly decrease the phosphorylation of GSK3α regardless of tumor types. (**E**) and (**F**) Comparison between the matched pairs of A549 and A549/SRFres tumors reveals significant increase in MMP9 expression in sorafenib-treated A549/SRFres tumors, and in the phosphorylation of SRC in dasatinib-treated A549/SRFres tumors. Error bars are SD. *P < 0.05 and **P < 0.01 using Kruskal-Wallis one-way analysis of variance on ranks followed by the post-hoc Kruskal-Wallis multiple comparison z-value test. +P < 0.05 compared with the counterpart A549 xenografts using the paired sample *t* test.